University of Stavanger

Faculty of Science and Technology

MASTER'S THESIS

Study program/ Specialization: MSc Petroleum Engineering/ Reservoir Engineering	Spring semester, 2012 Restricted access
Writer: Kanatbayev Maxym	..... (Writer's signature)
Faculty supervisor: Professor Svein M. Skjaeveland External supervisor(s): Dr. Øivind Fevang	
Title of thesis: Gas Condensate Field Performance Theory vs Practice	
Credits (ECTS): 30	
Key words: Gas-condensate reservoir Historymatching Well Deliverability Black-Oil Model Condensate Impairment Three-zone theory Multiphase Pseudopressure Function Steady-state liquid saturation PVT analysis	Pages: 59 + enclosure: 14 Stavanger, 08 June/2012 Date/year

Frontpage for master thesis
Faculty of Science and Technology
Decision made by the Dean October 30th 2009

Abstract

This report presents a study on how to represent wells in numerical simulation of a coarse-gridded, full-field study of a lean gas condensate reservoir. A "black oil" (formation volume factor representation of fluid properties) model had been historymatched by comparing tubing head pressures as well as adjusting the well deliverability by multipliers on the well productivity indexes, the "WPI Mult" approach. The objective of this work is to investigate how the historymatching of well deliverability approaches has an impact on the well flowing oil-gas ratio in original lean, fictitious medium and rich gas-condensates reservoirs.

Alternative well deliverability approaches investigated are called "Perm Mult" and "Fault Mult" with adjustment of permeability or transmissibility of numerical blocks surrounding the well blocks. The condensate impairment to the gas flow is well-known issue in gas-condensate fileds, but it is not accounted in a coarse-gridded model. The behavior of the important Region 1 and the change in the size of Region 1 are observed in well grid-cell and neighbouring grid cells. The steady-state liquid saturation is seen in Rich gas-condensate behavior after 5 years of production. Instead of tuning fluid properties to obtain a reasonable match between the measured oil-gas ratio and the simulated one, it is proposed to consider alternative well deliverability approaches.

Acknowledgements

I would like to express my sincere gratitude to my advisors, Professor Svein M. Skjaeveland and Dr. Øivind Fevang, for their support and guidance throughout this work. They have both always been available to answer my questions. Their great patience and encouragement helped me to finish this wok.

I would also like to give my sincere thanks to North Africa and Middle East team in Statoil, specially to Aissa for their gratitude and friendly environment have been shown during this work.

Special thanks also go to my parents and wife for their moral support and encouragement and all of my friends at UiS for making my stay at Stavanger memorable.

Table of Contents

List of Tables

List of Figures

Chapter 1

Introduction

Gas condensate reservoirs are mostly different from the black, volatile oil and gas reservoirs because of their complexity and less understandable phase and fluid behavior in the reservoir. The reservoir performance of gas condensate fluid behavior is widely addressed in many published papers to improve efficiency of the gas condensate reservoirs.

Liquid dissolved in natural gas at the initial reservoir conditions where the bottomhole pressure is above the dewpoint pressure is characterized by a single phase flow behavior which is not problematic issue for reservoir engineering team. However, complexity of phase and fluid behaviors can be addressed when the bottomhole pressure reduces below the dewpoint pressure. The accumulation of condensate close to the well bore can significantly reduce surface gas production rate by the reduction in gas relative permeability depending on the richness of gas condensate fluid. This phenomenon is known as condensate blockage.

The impact of condensate blockage on the well deliverability has been the subject of research. Generally, based on technical papers the main parameters that affect well deliverability in low permeable gas condensate reservoirs can be classified as: 1. the pressure drawdown strategy; 2. well completion type (vertical or deviated wells); 3. reservoir heterogeneity; 4. reservoir structure type (non-fractured or naturally fractured); 5. completion fluids; 6. relative permeabilities and saturation; 7. phase diagram and compositional fluid change; 8. fluid properties change; 9. the dependence of the relative permeability on capillary number; 10. the effect of wettability; 11. the effect of skin factors; 12. grid block size etc. Various well testing, laboratory and numerical simulation studies for different type of gas-condensate systems confirmed that the condensate accumulation does exist and the effects of the above-mentioned parameters on well deliverability have been observed.

The liquid accumulation around the wellbore was confirmed by the case studies of Deddy, et al. (1994). They pointed out that even with a fairly lean gas, liquid accumulation reduced individual well productivities by about 50% and productivity does not significantly improve until revaporization begins immediately around the wellbore, but revaporization process is

not relevant in the actual field study case. The potential for significant losses in gas recovery for initial permeability-thicknesses below 1000 md-ft over a range of condensate yields (Barnum et al., 1995). However, Du et al. (2004) showed that both high and low-permeability reservoirs are susceptible to condensate banking impact, but well the deliverability of low permeability gas reservoir losses more than high permeability gas reservoir.

Fevang and Whitson (1995) accounted for the appearance of a transition zone. The three-region theory is widely used to correctly simulate fluid behavior around the wellbore. The gas condensate well deliverability can be accurately calculated by using the multiphase pseudopressure function which captures a transition zone and accounts for the improvement in simulation models. Singh and Whitson (2008) confirmed that three-region theory proposed by Fevang and Whitson (1995) is valid and accurate for layered systems with significant heterogeneity, with and without capillary number modification of relative permeabilities for widely-ranging fluid compositions in each layer.

The gas-condensate well-testing study of Al Ismail (2010) also confirmed that the three-zone preudopressure is capable of representing the model pressure-saturation relationship and hence, estimating both permeability and mechanical skin accurately. The accurate modeling of gas condensate banking simulated by three-zone theory was summarized by Lee et al. (1998). However, Roussennac (2001) concluded that the steady-state and the three-zone multiphase pseudopressure are not robust to errors in the gas-oil ratio, the fluid sampling and the relative permeability. Consequently, even small errors in the gas-oil ratio lead to large error in the estimation of parameters when using the three-zone method (the steady-state method does not use the GOR information), but it is not confirmed by Fevang et al. (1995).

The dependence of relative permeability curves on interfacial tension and flow rate has been addressed in many papers. Blom and Hagoort (1997) concluded that the region where gas condensate relative permeability functions change from traditional immiscible curves to miscible straight lines is in the vicinity of the well bore. In addition, they pointed out that in tight reservoirs well impairment can be calculated using immiscible relative permeability curves (Corey functions), while in highly permeable reservoirs well impairment may be overestimated when using immiscible curves. Furthermore, near-critical relative

permeability and non-Darcy or inertial resistance are strongly coupled and condensate drop-out aggravates the inertial pressure losses (non-Darcy flow) (Blom and Hagoort, 1998).

Whitson and Fevang (1997) proposed that including the capillary-number, which defines the combined effect of velocity and gas/oil interfacial tension (IFT) on relative permeability, dependence on relative permeabilities within the three-zone pseudopressure function gives more accurate estimation of near-well pressure losses in coarse-grid simulators. Moreover, they pointed out that the effect of capillary number on gas-oil relative permeability can result in a significant improvement in gas relative permeability and thereby reduce the negative impact of condensate blockage. The validity of an empirical model proposed by Fevang and Whitson was also confirmed by Blom and Hagoort (1998). Non-Darcy flow is also typically less important than the relative permeability changes and high capillary numbers near the wells significantly increase the relative permeability, and thus, the production rate of the well increases (Chowdhury et al., 2008).

According to Du and Guan (2004), the PVT properties of the fluids have a large impact on gas condensate well deliverability loss. Therefore, the higher the liquid yield of gas, the larger the condensate banking effects, which results in the larger the well deliverability loss.

The wettability effect on the gas well deliverability is also an important issue that needs to be addressed. Li et al. (2000) and Al-Anazi et al. (2007) summarized that wettability alteration to intermediate gas wetting reduces critical condensate saturation dramatically, irrespective of gravity and interfacial tension and the most effective method for increasing gas well deliverability may be the alteration of wettability around the wellbore.

The different reservoir structure type has a significant impact on the well deliverabiity. Baig et al. (2005) pointed out that the fractured well, in this low permeability reservoir, has a higher productivity than the non-fractured well and recommended improvement in productivity can be achieved by increasing the length of the fracture up to a practical fracture half-length limit. In addition, they concluded that vertical and lateral heterogeneities results in irregular and complex condensate bank shapes.

The completion fluids showed a negative impact on gas relative permeability. The gas PI was reduced by more than 50% due to liquid entrapment (Al-Anazi et al., 2005).

All above condensate-banking related papers are summarized to understand the behaviour of gas condensate flow in the vicinity of the well. The condensate impairment to the gas flow is well-known issue in gas-condensate fileds, but it is not accounted in a coarse grid model.

To accurately model gas-condensate fluid behavior and capture condensate banking phenomena in the vicinity of the well it is advised to select reasonable grid block size. It is stated by Fevang et al. (1995) that the multiphase pseudopressure method treats the more important Region 1 accurately in coarse grid simulation. They also claimed that the size of the well grid-cell must be chosen properly in order not to overestimate pressure losses in Region 1.

The comparison of the Modified Black-Oil and compositional approach in full-field simulation studies was made in some papers. According to Ahmed et al. (2000), the MBO approach proved to be sufficient for modeling gas condensate behavior below the dew point and instead of using a fully compositional approach and it was allowed a rapid history match of the field performance. It is proposed by Fevang et al. (1995) that a modified oil viscosity should be used in Black-Oil model in order to obtain in the same result as a fully compositional Equation of State (EOS).

Few researchers have addressed the historymatching problem in the vicinity of the well in gas-condensate field. We propose to investigate how the historymatching of well deliverability approaches has an impact on the well flowing oil-gas ratio before starting to tune fluid properties in order to obtain a reasonable match between the measured oil-gas ratio and the simulated one.

Chapter 2 mainly discusses how the gas condensate characterization may be described by ternary diagram and phase and equilibrium behavior of fluid flow in the gas-condensate reservoir. Moreover, based on three-zone model buildup behavior and fluid flow regimes of gas condensate are briefly discussed. In addition, the appearance of condensate blockage and change in compositional phase behavior around the wellbore are also introduced. The importance of coexistence of flow regions based on the pressure drop strategy and the multiphase pseudopressure function proposed by Fevang et al. (1995) are summarized in this chapter.

Chapter 3 introduces the purpose of different well deliverability (WD) approaches and summarizes the results of numerical simulation studies for lean, medium and rich gas condensate systems in the low, medium and high permeability block layers.

Chapter 4 summarizes the main conclusions and further works that need to be undertaken to accomplish the objective of these studies.

1.1. The Problem Statement

The objective is to check out three different well deliverability (WD) approaches in Eclipse of a gas condensate well and its surroundings for historymatching a gas condensate reservoir. A full field B-O model of In Amenas field with standard coarse grid and original lean gas-condensate reservoir is given by Statoil to carry out numerical simulation studies. The historymatching of two Tg303bis and Tg307ter is already done in the existed model by WPI Mult approach, which is explained below. It is suggested that "Perm Mult" and "Fault Mult" approaches can also be used for historymathing by adjusting the reservoir data such as the permeability or transmissibility factors in the vicinity of the well. Furthermore, there exist measured data only from the lean gas condensate (LGC) reservoir and it is difficult to say that one of these three approaches is “the best” to use for the lean GC reservoir because of the lack of the measured well flowing OGRs in the B-O model by wells. However, all of three WD approaches are important for the historymatching procedure. For the medium and rich gas condensate fictitious reservoirs, for which there is no measured data, the three approaches are sensitive to the richness of the condensate. In addition, the gas rate is fixed while the condensate rate is increasing in all of gas-condensate fluid systems.

1.1.1. Well productivity approaches

Three different well productivity approaches such as improved PI, altered permeability and introduced fault with transmissibility factors are considered.

- PI multiplier (WPI Mult approach) – can be used to multiply the connection transmissibility factors of selected well connections by a specified value (Eclipse Reference Manual, 2010). In Eclipse, it is defined as the “WPIMULT” keyword and is simply called as a “base case”. In this particular study, “WPIMULT” keyword is already defined in existed B-O model by a specified value. A new adjustment is made by

totally replacing “WPIMULT” keyword with “Perm Mult” and “Fault Mult” approaches.

- Altered permeability (Perm Mult approach) – a factor which is used to alter the permeability in the vicinity of the well for historymatching procedure. In Eclipse, it is defined as “PERMX, Y or Z” under the “Multiply” keyword. In this particular study, the permeability values are improved or increased in all directions multiplied by the same value in the region around the well which is in turn defined with grid blocks 3 x 3 or 4 x 4 depending on the well completion type. For example: both Tg307ter and Tg303bis are horizontal wells and selected grid block size close to the well is 5 x 5 and 3 x 7 respectively.

- Introduced fault with transmissibility factors (Fault Mult approach) – The “MULTFLT” keyword can be used to modify the transmissibility (and diffusivity) across a fault previously defined using the “FAULTS” keyword (Eclipse Reference Manual, 2010). In this particular study, transmissibility factors are adjusted between two grid blocks in the outer boundary of the selected region close to the well and all faults are multiplied by the same value. The selected grid block size around the well is the same as in Perm Mult approach.

The selected blocks around of two Tg307ter and Tg303bis wells are clearly seen in the pressure depletion map, as shown in the green blocks in Fig. 1.1. As it is mentioned above, the condensate impairment is mainly occurred in the region around the well.

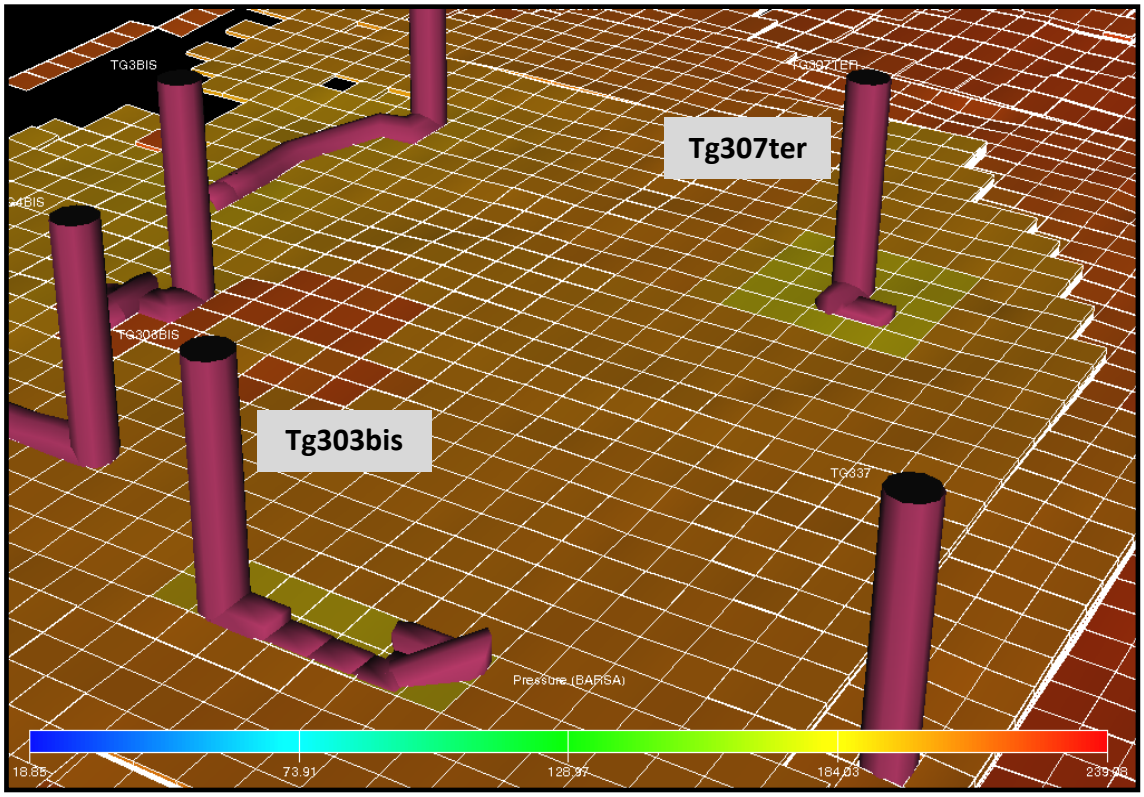

Fig. 1.1: The map of the block pressure depletion in Fault Mult approach

Chapter 2

Gas Condensate Flow Behavior

2.1. Gas Condensate Characterization

The main three classifications of petroleum reservoirs such as oil, gas condensate and gas are known. All fluid types can be differentiated depending on fluid properties and phase behavior in the reservoir. The most problematic fluid type is gas condensates which are mostly found between the critical and the cricodentherm temperatures. A single gas phase flow exists if the bottomhole pressure is above the dewpoint pressure. Low condensation formation in the reservoir can exist or relatively large amount of condensate can be produced at surface depending on the richness of the gas condensate if the bottomhole pressure is below the dewpoint pressure. Fig. 2.1 shows a ternary diagram of black oil, volatile oil, gas and gas condensate in mole percentage. Typical characteristics of hydrocarbons are given in Table 2.1

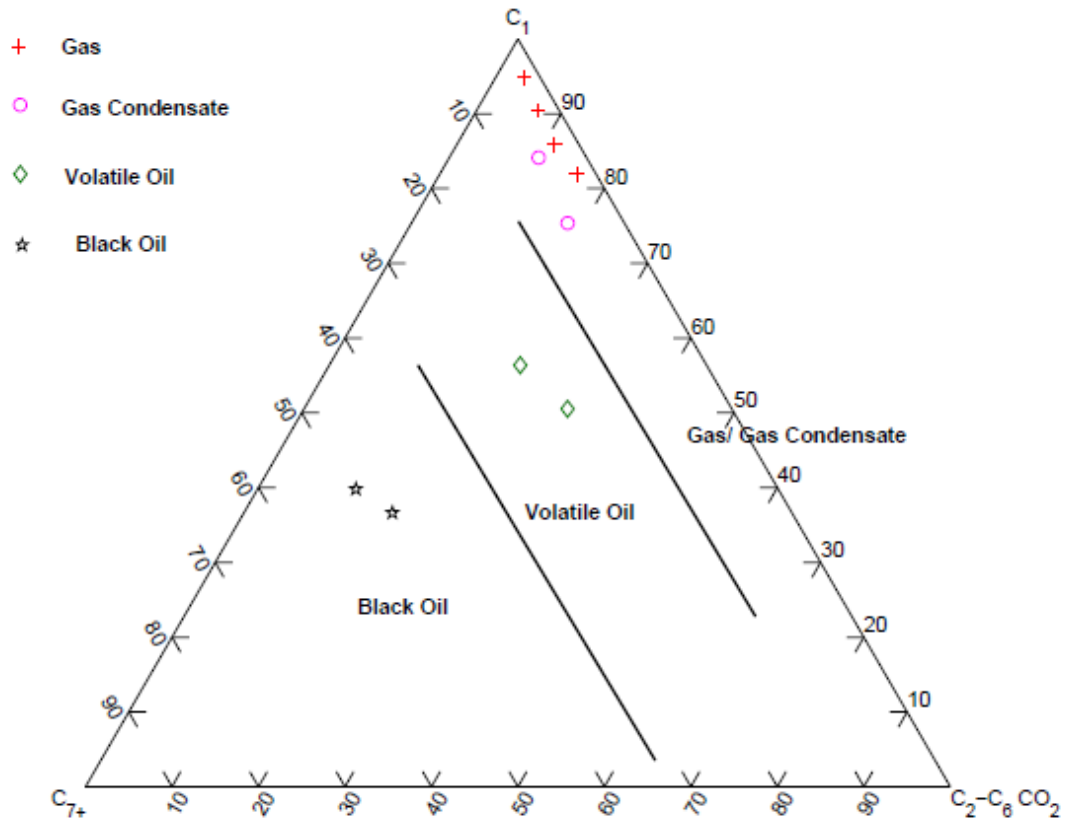

Fig. 2.1: Ternary visualization of hydrocarbon classification (Roussennac, 2001)

C_{7+} mole concentration in gas condensate is less than concentration of C_{7+} in volatile oil in the near critical region.

Table 2.1: Composition and properties of several reservoir fluids (Wall, 1982), mole percentage fractions

Component	Black Oil	Volatile Oil	Condensate	Gas
Methane	48.83	64.36	87.07	95.85
Ethane	2.75	7.52	4.39	2.67
Propane	1.93	4.74	2.29	0.34
Butane	1.60	4.12	1.74	0.52
Pentane	1.15	2.97	0.83	0.08
Hexane	1.59	1.38	0.6	0.12
C7+	42.15	14.91	3.80	0.42

2.2. Gas Condensate Flow Behavior

2.2.1. Phase and Equilibrium Behavior

A pressure-temperature diagram to illustrate gas condensate phase behavior is shown in the Fig. 2.2. According to the phase envelope, if the bottomhole pressure is above the dew-point pressure in the critical-cricondentherm temperature interval which is a B-B1 path, so a single gas phase exists in the reservoir. Reduction in the bottom-hole pressure results in liquid condensation from the gas which is along a B1-B3 path. A two-phase system is formed in the reservoir where liquid will start flowing when it reaches the critical condensate saturation. At some point which is likely a point B2 in the Fig. 2.2, the maximum liquid dropout occurs in the reservoir followed by revaporization of condensate into the gas which is found at low pressure.

According to Fig. 2.3, the behavior of gas-condensate systems changes depending on the richness of the reservoir fluid. The highest liquid dropout is occurred in the rich GC, showing almost 25%, while in the lean GC there is no huge liquid dropout because the fluid system mainly consists of the lighter hydrocarbon components and less heavier components. The productivity ratio of rich GC system is substantially declined as the pressure is below the dewpoint pressure of the original reservoir, whereas it is also reduced dramatically in lean GC, but the pressure can still be above the initial dewpoint pressure.

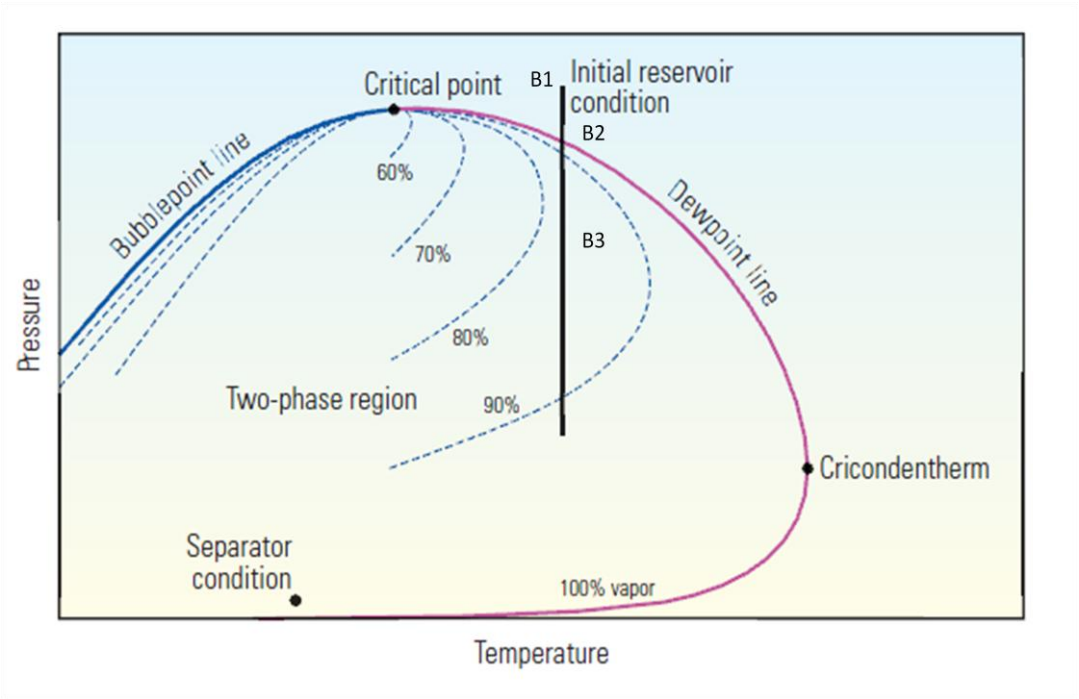

Fig. 2.2: Phase diagram of a gas-condensate system (Fan et al., 2005)

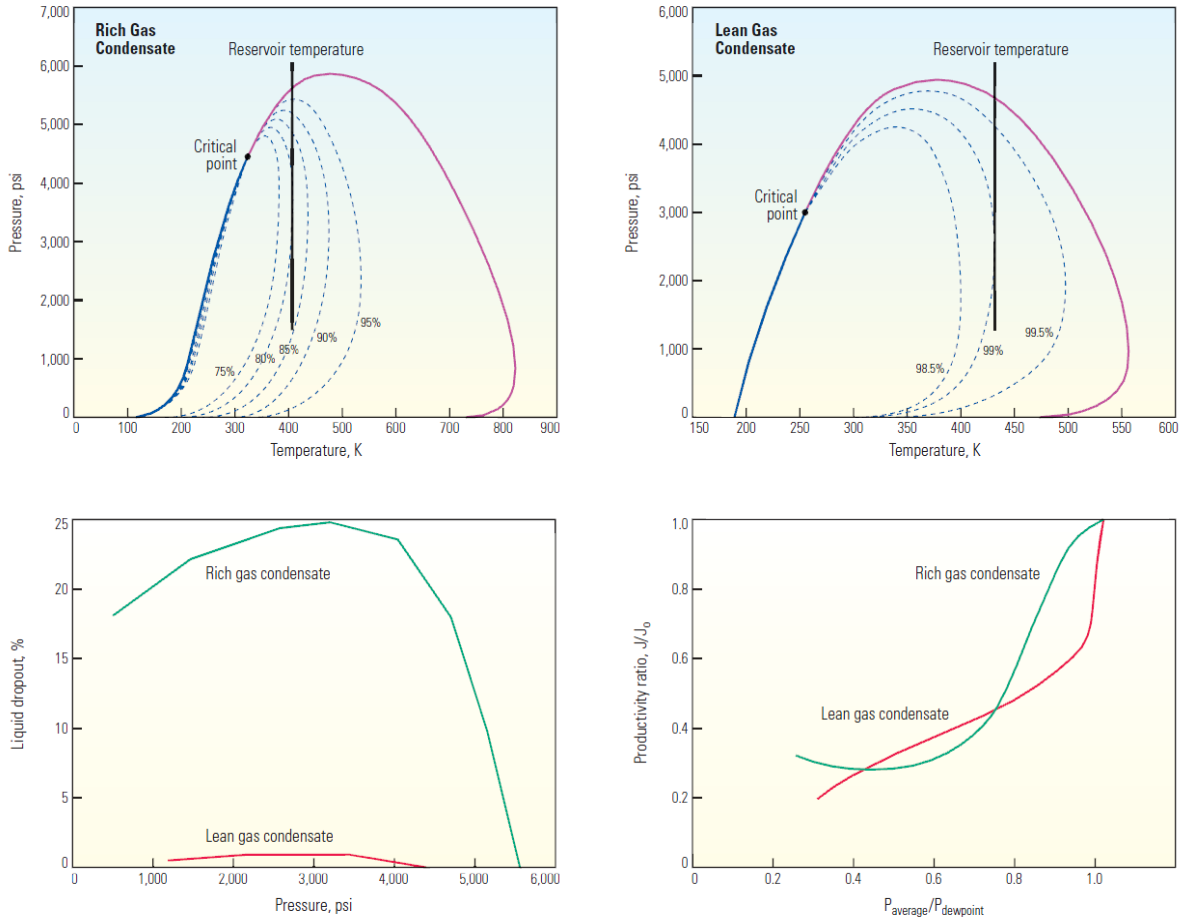

Fig. 2.3: The behavior of rich and lean-condensate (Fan et al., 2005)

2.2.2. Build up Behavior and Flow Regimes

Fluid flow behavior of gas condensate in the reservoir can accurately be estimated by the three-zone model proposed by Fevang et al. (1995):

- **Region 1** – the region around the well where the bottom-hole pressure is far below the dew-point pressure.

If the liquid saturation exceeds the critical condensate saturation, both condensate and gas can flow simultaneously. It is believed that the flowing gas-oil ratio (GOR) is constant throughout Region 1 which means that the produced wellstream mixture is the same as a single-phase gas entering Region 1. In addition, the pressure drawdown close to the well is higher than in other regions, consequently the condensate saturation will increase as both condensate and gas flows towards the well.

If the pressure drawdown increases over time, the liquid saturation around the wellbore will start to increase causing the flowing OGR to decrease. Liquid saturation towards the well can also decrease as a function time and pressure depicted in Fig. 2.4. However, the drop in liquid saturation can be observable only after a period of production time when a steady-state is reached. The main reason of reduction in liquid saturation is the composition of a single-phase phase entering Region 1 which will become leaner and leaner dropping out more heavy components.

Furthermore, the size of Region 1 will expand as a function of time and pressure drawdown. If the BHFP is below the initial dewpoint pressure, the minimum size of Region 1 will be detected at earlier stage and Region 2 will gradually be occupied by Region 1. Depending on PVT and fluid properties the size of Region 1 will vary displacing the lowest possible size of Region 1 at earlier stage of production in the rich gas condensate leaving the medium gas condensate behind followed by the lean gas condensate. The size of Region 1 in the medium and rich gas condensates will expand as a function of time and pressure drawdown.

The condensate blockage is a main source of flow resistance and the relative permeability and liquid saturation are a function of time and the pressure drawdown in this region which depends on the PVT and fluid properties of a single-phase gas leaving Region 2.

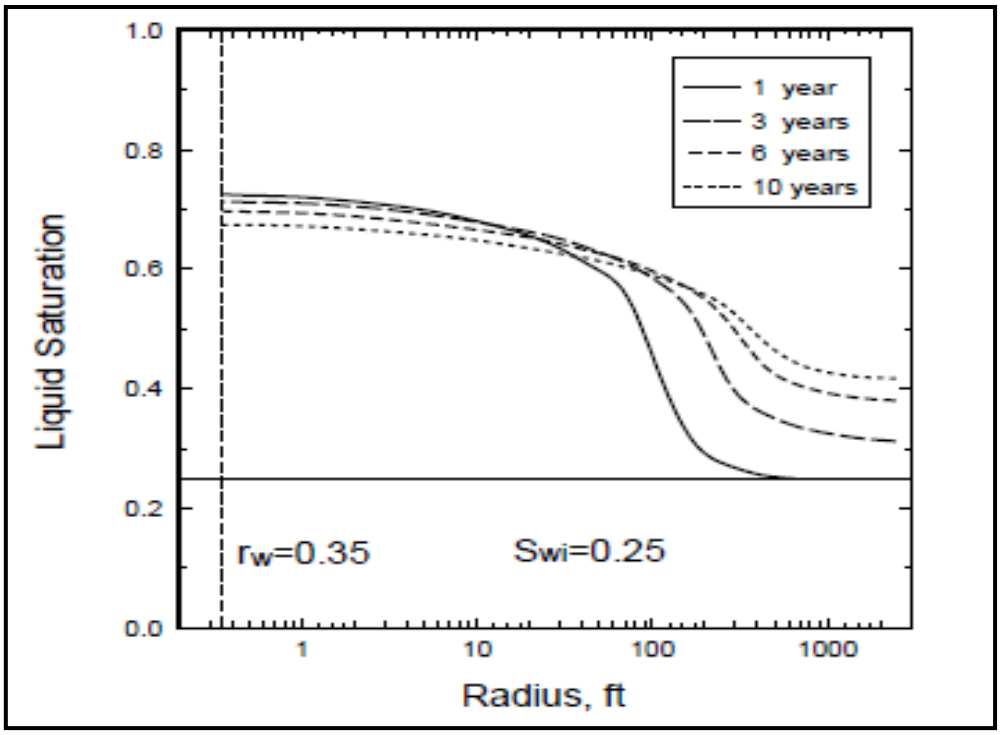

Fig. 2.4: Liquid saturation as a function of radius at different stages of depletion (Fevang, 1995)

- **Region 2** – is a condensate blockage region where condensate phase is immobile.

The accumulation of condensate is not sufficient to be mobile because it has not reached the critical condensate saturation. The size of Region 2 reduces as a function of time, while Region 1 expands gradually because of mobile gas in Region 2 becomes leaner and leaner with leaving the intermediate and heavy components behind. At the outer Region 2, where the first droplets of liquid start to condensate from gas, the pressure equals to the initial dew-point pressure of the reservoir. As the condensate buildup occurs in Region 2, a short period of transition time is needed to build up Region 1.

The condensate buildup is mainly caused by: 1. the bulk volume depletion of the reservoir; 2. the pressure gradient imposed on the flowing reservoir gas within Region 2 (Fevang et al., 1995). If the buildup of condensate is caused by the pure pressure depletion, the condensate saturation is calculated from the liquid dropout curve from a constant volume depletion (CVD) experiment, corrected for water saturation (Whitson et al., 1983).

The appearance of Region 2 is essential for appropriately defining flow behavior of the reservoir fluid because the producing OGR is leaner than calculated by a simple volumetric

material balance (CVD experiments) which can result in the overestimation of deliverability loss, mostly at earlier time of depletion (Fevang, 1995).

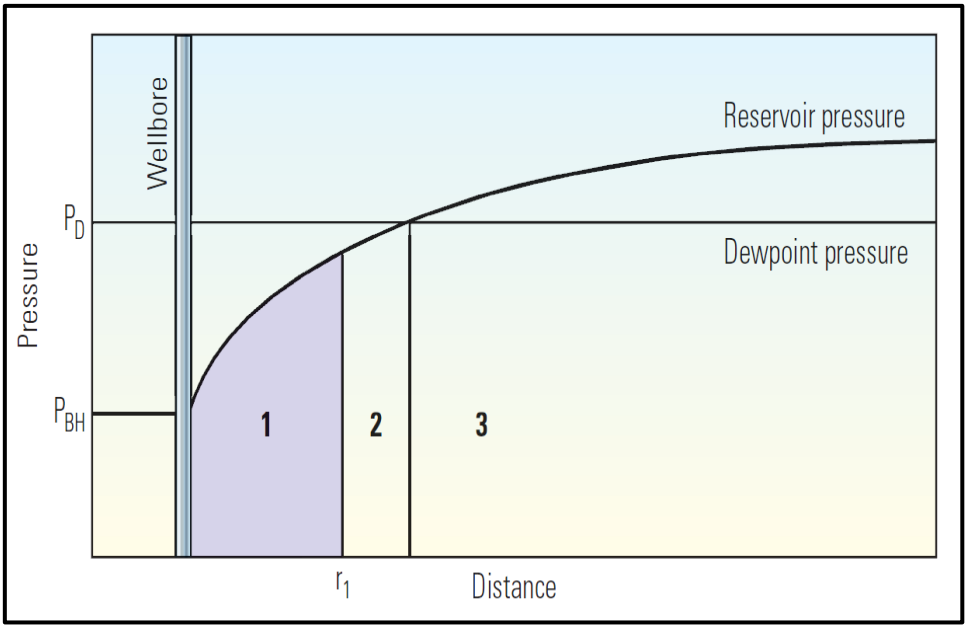

Fig. 2.5: Three reservoir regions (Fan et al., 2005)

- **Region 3** – an outer region of the reservoir where the pressure is above the dew-point pressure. The well deliverabiltiy equation of Region 3 is treated as a single-phase gas flow.

According to Ayyalasomayajula et al. (2005), the simulated condensate bank after ten years of production ranges from 40 to 225 feet, with the bank being larger in the higher permeability layers. The size of the condensate also depends on the pressure drawdown strategy. If the BHFP is reduced fast, consequently the reduction in gas relative permeability results in the more condensate buildup and a more amount of trapped heavy-components around the wellbore. The boundaries between the regions are not stable and change as functions of time and pressure drawdown. Depending on the PVT and fluid flow properties, reservoir characteristics, pressure drawdown strategy etc., the boundaries of each region can be estimated or simulated based on well testing and numerical simulation tools.

2.2.3. Condensate Blockage

The condensate blockage mainly occurs in Region 1 because condensate impairment restricts the flow of gas to the well. Depending on the richness of the gas condensate the relative permeabilities of gas and condensate change as a function of time and the pressure in Region 1 mainly contributes to condensate blockage.

It is believed that as the size of Region 1 increases because of gas entering Region 1 becomes leaner and leaner, the composition of gas condensate around the well bore changes significantly as a function of time and pressure. The existence of condensate blockage region will vary depending on richness of the gas condensate. In rich gas condensate reservoirs condensate blockage is an important phenomenon because of the highest liquid dropout which in turn serves as condensate impairment to the gas flow.

2.2.4. Condensate Phase Behavior Change

The phase envelope change is mostly observed in a PVT cell. The original reservoir phase envelope is one to the left in Figure 2.5. In a reality, the liquid drop-out in the reservoir is much higher than shown in the phase diagram.

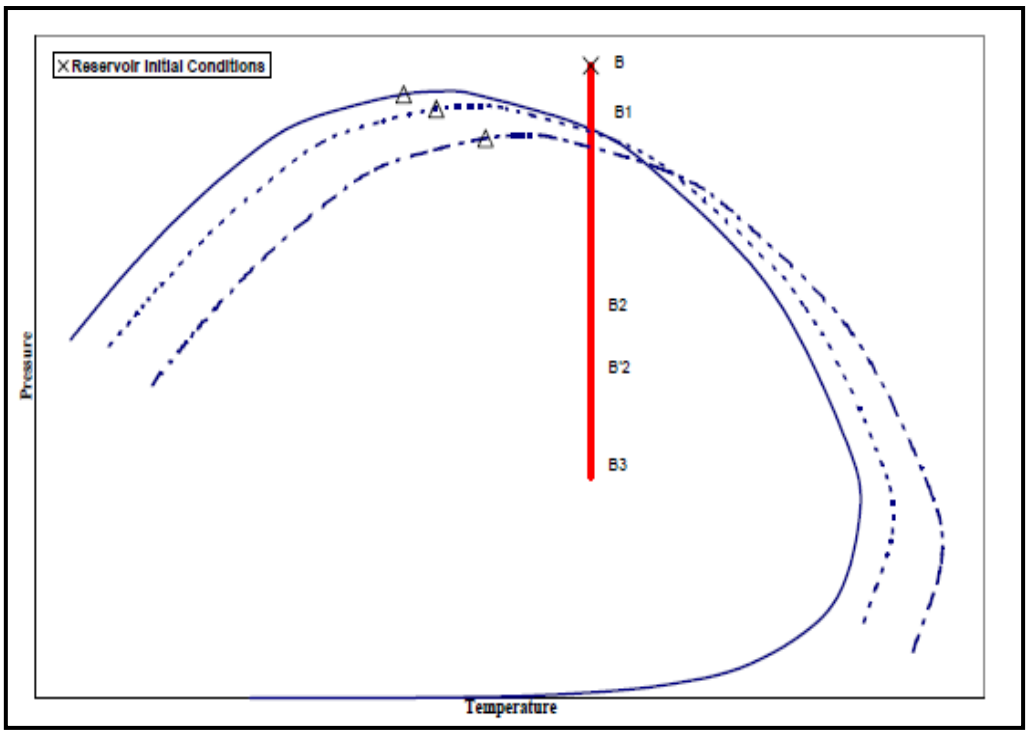

Fig. 2.6: Shift of phase envelope with compostional change (Roussennac, 2001)

The heavier components of the gas condensate system is mainly concentrated to condensate liquid, while the leaner components of gas are produced at surface it is mainly part of the intermediate component. Consequently, the shift of phase diagram is observed throughout reservoir performance. The mobility of the gas is improved with respect to the condensate by the viscosity of the liquid which becomes higher and the viscosity of gas becomes lower. It is not unusual that a retrograde-condensate composition would exhibit a bubble-point pressure if the reservoir were repressurized (Lal, 2003).

2.3. Gas Condensate Well Deliverability

2.3.1. Coexistence of Flow Regions

Region 3 will only exist if the bottom-hole flowing pressure (BHFP) is above the initial dew-point of the reservoir according to the Table 2.2. However, this phenomenon is not common for gas condensate because the pressure drop around the wellbore will increase dramatically depending on the richness of the condensate.

Region 1 and Region 2 will co-exist if the reservoir pressure falls below the dew-point pressure which results in the absence of Region 3. It is suggested that all three regions may co-exist together if the average reservoir pressure is still above the dew-point pressure in Region 3 and the liquid starts to condense from gas below the dew-point in Region 2 which in turn will create Region 1 after a short transition period. The flow regions will always vary depending on the richness of gas condensate, tubing size, surface well regimes, target production rate, field development plans etc.

Table 2.2: Coexistence of flow regions (Fevang et al., 1995)

Coexistence of Flow Regions			
	$P_{wf} > P_d$	$P_R < P_d$	$P_{wf} < P_d$ and $P_R > P_d$
Region 1		X	X
Region 2		(X)	(X)
Region 3	X		X
X exist and (X) may exist			

2.3.2. Multiphase Pseudopressure Function (MPF)

Fevang and Whitson (1995) proposed a simple multiphase preudopressure function based on observations of the three flow regions for many gas condensate systems in term of *Black-Oil* PVT and fluid properties is written as:

$$\Delta P_P = \int_{P_{wf}}^{P*} \left(\frac{k_{rg}}{B_{gd} \cdot \mu_g} + \frac{k_{ro}}{B_o \cdot \mu_o} \cdot R_s \right) dp + \int_{P^*}^{Pd} \frac{k_{rg}}{B_{gd} \cdot \mu_g} dp + k_{rg}(S_{wi}) \cdot \int_{P_d}^{P_R} \frac{1}{B_{gd} \cdot \mu_g} dp \quad 2.1$$

The first term of the above equation is related to Region 1, where both condensate and gas flow simultaneously, the second term is in Region 2 where condensate is immobile and the last term is in Region 3 where a single-phase gas flows.

The compact form of pseudopressure function is written as:

$$\Delta P_P = \int_{P_{wf}}^{P_R} \left(\frac{k_{rg}}{B_{gd} \cdot \mu_g} + \frac{k_{ro}}{B_o \cdot \mu_o} \cdot R_s \right) dp \quad 2.2$$

where: p_{wf} is the flowing bottom-hole pressure, p^* is pressure at outer boundary of Region 1, p_d is a initial dew-point pressure at outer boundary of Region 2 and p_R is the original reservoir pressure. Consequently, the gas condensate rate equation is given as:

$$q_g = C \cdot \Delta P_P, \quad 2.3$$

where

$$C = \frac{2\pi a_1 kh}{ln\frac{r_e}{r_w} - 0.75 + s}, \quad 2.4$$

and the a_1 and C parameters are the same as for gas rate equation in Eq. 2.4.

Chapter 3

The field overview

The In Amenas Gas Condensate project is an important initiative in the development of Cambro-Ordovician and Devonian (subordinate) gas reservoirs of the Illizi basin. The project area is located in the southern portion of the Illizi basin, approximately 850 km south of Hassi Messaoud and 40 km southwest of the town of In Amenas. It consists of two components: Cambro-Ordovician reservoirs in the Tiguentourine and La Reculée fields and Devonian reservoirs in the satellite fields (Hassi Farida, Ouan Taredert, and Hassi Ouan Abecheu), lie immediately to the southeast, as depicted in the Fig. 3.1. The Cambro-Ordovician reservoirs of the Tiguentourine and La Reculée fields contain at least 6.1 TCF GIIP. Based on a 75% recover factor from reservoir simulation and assuming 250 psi inlet compression, wet-gas reserves are estimated at 4.6 TCF for Tiguentourine. Reserves for the Devonian satellite fields is estimated at approximately 0.8 TCF of wet gas, for a combined, cumulative wet-gas reserves of 5.4 TCF. For a 20-year production profile, the reservoirs are expected to produce at least 5.1 TCF. (In Amenas Development Plan, 2002). In Amenas field crude characteristics are listed in the Table 3.1.

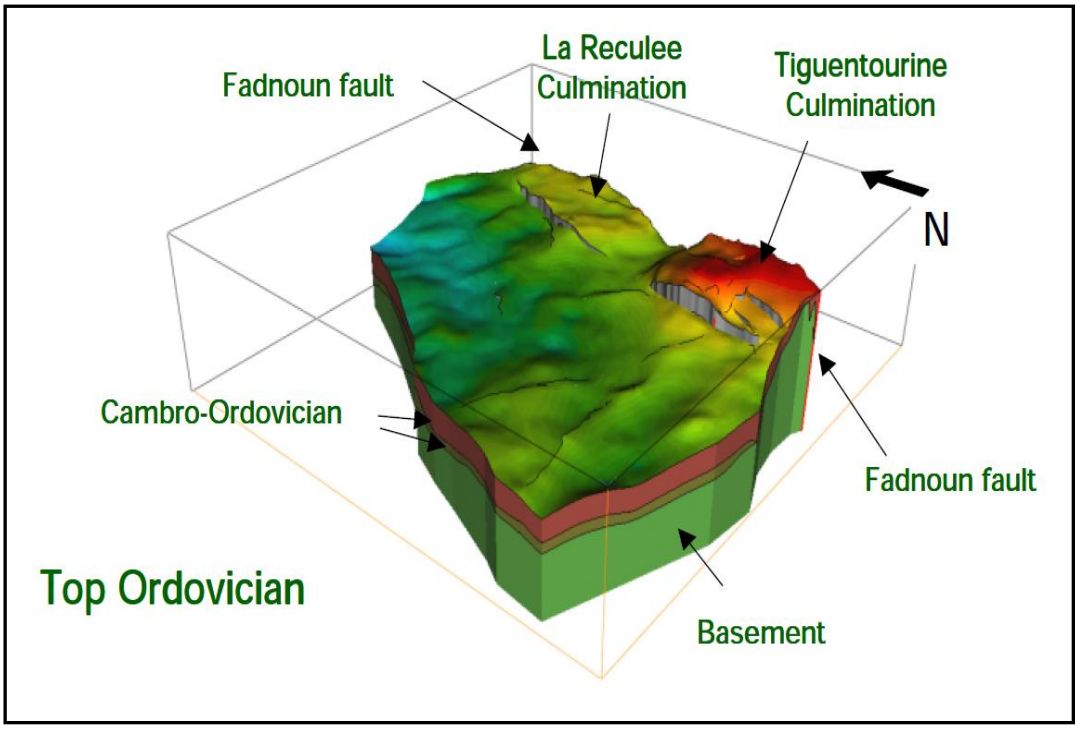

Fig. 3.1: The reservoir view of Tiguentorine and La Reculee structures

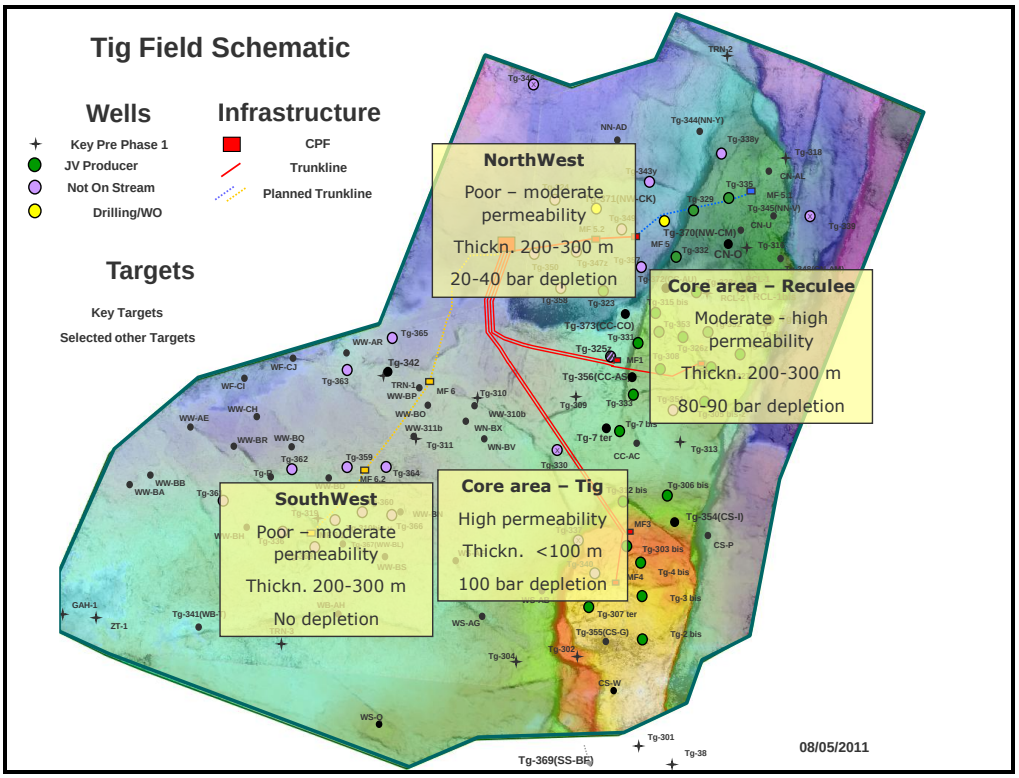

Fig. 3.2: The schematic view of Tiguentorine and La Reculee structures

The Tiguentourine structure is one of the main core areas. As shown in the Fig. 3.2, the permeability is high and thickness is below 100 m. The reservoir is depleted at almost 100 bar by June 2011. The La Reculee structure characterizes moderate to high permeability and thickness 200-300 m with 80-90 bar reservoir depletion. The permeability of North-West and South-West structures is poor to moderate with 200-300 m thickness, but the former reservoir is depleted at 20-40 bar. The total 25 wells are on production. The main key figures of the field are: initial reservoir pressure - 226 bara; GIIP – 500 BCM (18 TCF) and plateau Rate – 25.8 MMSm^3/d.

Table 3.1: In Amenas field crude characteristics

API	68.7°
S.G.	0.7069
Sulphur, mass%	0.001
Pour Point	< -45 °C
Nickel, wppm	< 0.1
Vanadium, wppm	< 0.1
Visc. (20°C), cSt	0.6

3.1. Selected wells characteristics

In a coarse grid numerical simulation, two Tg303bis and Tg307ter wells are selected to observe the impact of the historymatching on the flowing OGR. The low, medium and high permeability layers of the region close to the well are selected to ensure that the numerical simulation studies have been applied for all different type of layers.

Low permeability gas condensate reservoirs (< 1000 md-m) are characterized by complicated or unpredictable flow behavior in Region 1 (Barnum et al., 1995). The flow capacity of two wells is below 1000 md-m around the well grid-cell. The region around the well is a primary important when it comes to gas condensate reservoirs. As it is mentioned above, the WPI Mult approach is already used in the B-O model with the original lean gas condensate and the historymatching is also done by applying the WPI Mult approach. The values of WPI Mult approach in two Tg303bis and Tg307ter wells are 0.07 and 0.23 respectively. It is advised that if the values of WPI Mult approach is above 0.3, it is preferred not to consider at all because of the sufficient and potential gas rate at surface.

In addition, the numerical simulation studies of Tg303bis and Tg307ter wells are also carried out for low, medium and high permeability layers in the selected block distance, as shown in the Fig. 3.2 and Fig. 3.3. The results of simulation studies are only shown for Case 1, in particular, in Tg307ter well the layer 7 out of 46 in k direction is selected, while in Tg303bis well the layer 11 out of 46 in k direction is chosen to observe any changes in the block parameters in the selected distance. The results of Case 2 and Case 3 are also discussed in the results part of each well.

Table 3.2: The block permeability (mD) distribution over the selected distance, Tg307ter

Distance, m		100	200	300	400	500	600	700
# Case	*i* and *j* directions / *k* direction	42 119	43 119	44 119	45 119	46 119	47 119	48 119
Case 1	7	34.285	46.004	20.444	25.738	23.019	22.576	38.252
Case 2	14	0.2875	0.4550	0.4403	0.2945	0.2036	0.3175	0.327
Case 3	16	507.92	109.93	99.253	192.1	173.85	130.21	77.674

Table 3.3: The block permeability (mD) distribution over the selected distance, Tg303bis

Distance, m		100	200	300	400	500	600	700
# Case	*i* and *j* directions / *k* direction	47 101	47 102	47 103	47 104	47 105	47 106	47 107
Case 1	11	171.48	222.76	217.65	189.96	185.6	263.79	299.06
Case 2	13	0.6848	0.416	0.3726	0.2982	0.5699	0.6948	1.505
Case 3	7	29.653	35.548	65.896	2.3027	66.165	141.46	134.98

3.2. Black-Oil Properties

Numerical simulation studies are commenced by original lean gas condensate (LGC). The Lean GC PVT and fluid properties are already defined in the existed Black-Oil (B-O) model. The Medium (MGC) and Rich gas condensate (RGC), for fictitious reservoirs, are separately added to the B-O model to observe the impact of historymatching of the different WD approaches on the flowing OGR.

The Black-Oil approximation assumes that PVT behavior of reservoir oil can be modified by "two components" denoted "oil" and "gas". It is assumed that they are fixed composition with constant mass and density. The reservoir liquid and vapour streams are then taken to stock tank conditions via separator network (Roussennac, 2011). The reservoir fluid is basically described by the following variables:

- **Solution oil-gas ratio r_s and solution gas-oil ratio R_s**

Fig. 3.3. and 3.4 represent the relatonship of the input solution oil-gas ratio and solution gas-oil ratio to pressure. The solution oil-gas ratio decreases gradually if the pressure is below the dewpoint pressure of the reservoir. The reason is that when the condensate critical saturation is reached in Region 1 after a short transient time or after formation of the Region 2 of the condensate accumulation, both oil and gas flow simultaneously within Region 1 which in turn causes the reduction in the solution oil-gas ratio and gas-oil ratio.

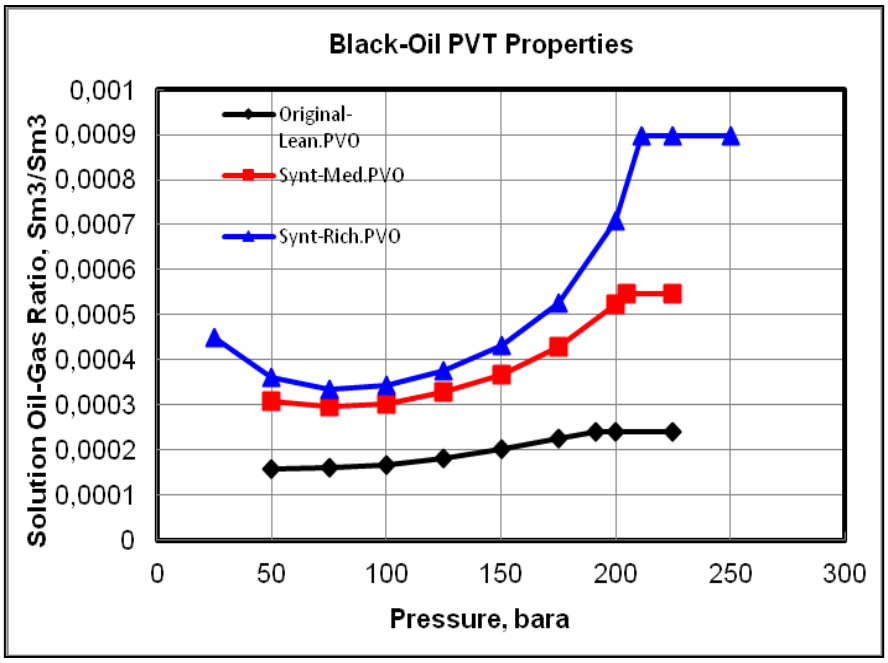

Fig. 3.3: The comparison of solution OGR vs. pressure between lean, medium and rich GCs

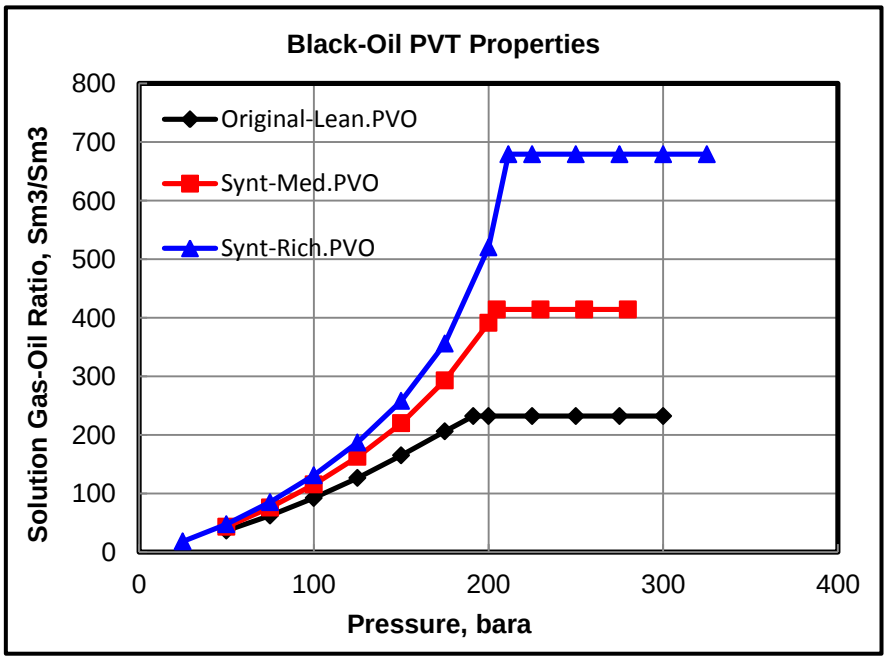

Fig. 3.4: Solution GOR by pressure depletion for lean, medium and rich GCs

It is believed that p^* must be equal the dewpoint of the producing wellstream as well as the dewpoint pressure of the gas leaving Region 2, since the flowing GOR is constant throughout Region 1. The multiphase pseudopressure method in a coarse gid simulation leads to reasonably accurate producing GOR compared with a fine-grid model and the behavior of Region 1 is also treated accurately in the well grid-cell (Fevang et al., 1995).

- **Formation oil factor B_g (for gas) and B_o (for oil)**

The relationship of oil and gas formation volume factors to pressure for Lean, Medium and Rich GC fluid systems in shown in A.1.1 and A.1.2 (Appendix A.1).

- **Oil and gas viscosity**

The coefficient of viscosity is a measure of the resistance to flow exerted by a fluid. Viscosity of oil, like other physical properties of liquids, is affected by both pressure and temperature. An increase in temperature causes a decrease in viscosity. A decrease in pressure causes a decrease in viscosity. A decrease in the amount of gas in solution in the liquid causes an increase in viscosity (William and McCain, 1990). This is related to the black oil fluid. However, the gas condensate reservoir can experience the same behavior because of formation of two-phase flow as the pressure is below the dewpoint pressure.

Fig. 3.5 and 3.6 show the relationship of the oil and gas viscosities to pressure at constant temperature for original lean, medium and rich gas-condensates. A reduction in pressure causes a decrease in oil viscosity as well as in gas viscosity. As the pressure is below the dewpoint pressure of the gas, liquid condenses from the gas leaving behind a free liquid in the reservoir and valuble medium and heavier components. There is an increase in oil viscosity below the dewpoint pressure of the reservoir, while gas becomes leaner and gas viscosity experiences a considereable decrease.

In Eclipse, oil and gas viscosities are both used as the input fluid properties. If the reservoir pressure is above the dewpoint pressure of the gas, there is just a single gas phase flow and viscosity of gas is used above the dewpoint pressure. If the pressure is below the dewpoint pressure, two-phase flow occurs and both oil and gas viscosities are used.

It is proven by Fevang et al. (1995) that a lower oil viscosity in the compositional simulation results in a lower oil relative permeability and lower oil saturation than in the black-oil simulation. Therefore, lower oil saturation results in higher gas relative permeability and improved well deliverability for the compositional simulation. Since the composition of gas and condensate gradually changes below the dewpoint pressure in the vicinity of the well, it is preferred to modify viscosities in the black-oil simulator taking into account the change in the compostion.

Fully compositional simulation is adequate for describing the behavior of gas condensate flow, the black oil properties are useful to compute the three-zone pseudopressure (Roussennac, 2011).

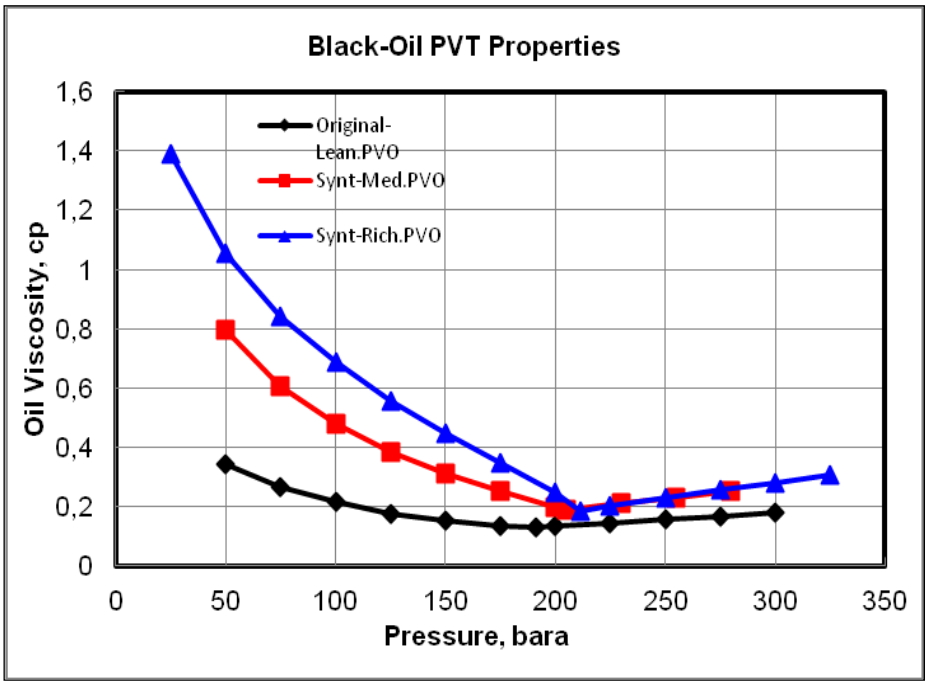

Fig. 3.5: The comparison of oil viscosity vs. pressure between lean, medium and rich GCs

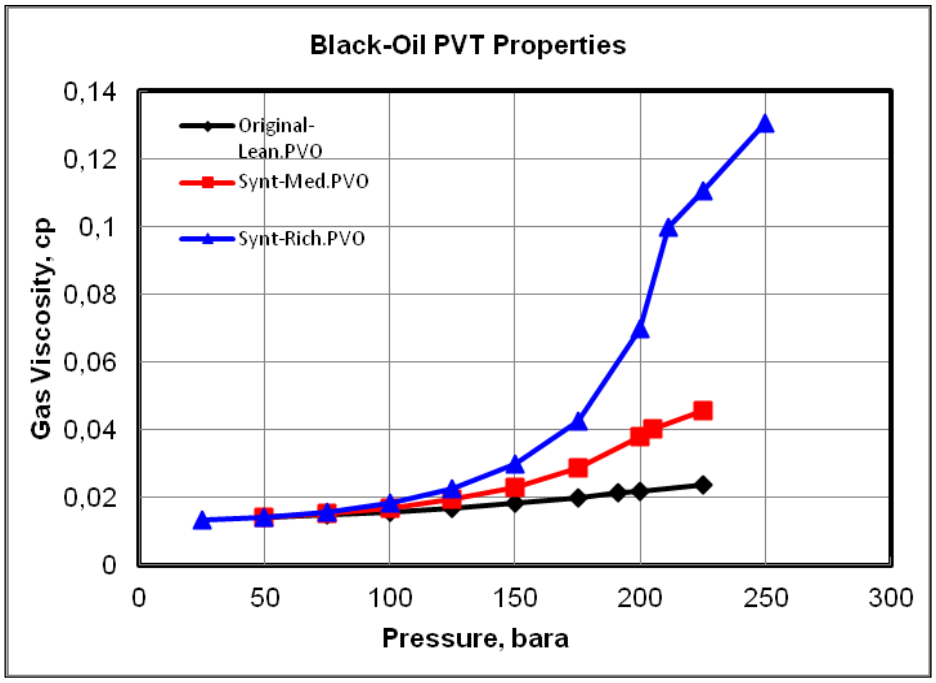

Fig. 3.6: The comparison of gas viscosity vs. pressure between lean, medium and rich GCs

Chapter 4

Well Deliverability Approaches

4.1. The Comparison of THPs in WPI Mult approach

A "black oil" model had been historymatched by comparing tubing head pressures as well as adjusting the well deliverability by multipliers on the well productivity indexes, the "WPI Mult" approach. The comparison of tubing head pressures (THP) between Lean, Medium and Rich GC systems in WPI Mult approach is shown in Fig. 4.1 for Tg303bis well and in Fig. A.2.1 (Appendix A.2) for Tg307ter well. The THPs of Medium and Rich GC in WPI Mult is simulated such that the THPs of Lean GC in WPI Mult approach is somewhat higher compared to Medium and Rich GC.

Vertical Lift Performance (VLP) curves of the original lean GC are used in numerical simulation for original Lean, Medium and Rich GC systems.

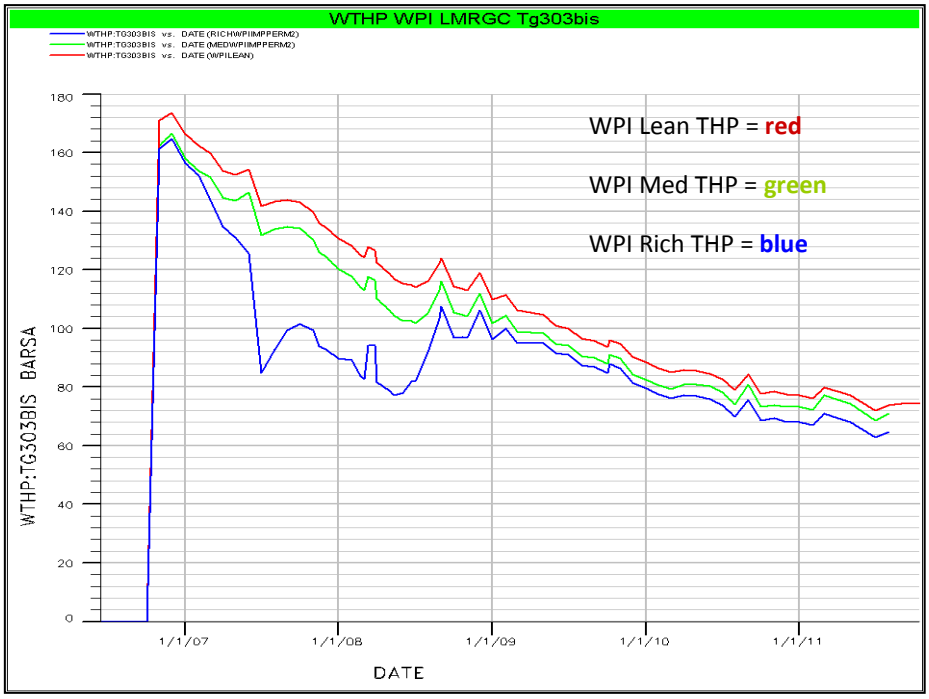

Fig. 4.1: The THPs of WPI Mult approach for lean, medium and rich GC, Tg303bis

4.2. Results for all fluid types

4.4.1. Tg307ter simulation result

Numerical simulation study is carried out by original Lean, Medium and Rich gas-condensates. In Lean GC, the overall trend of gas production rate at surface, which is solid brown curve depicted in Fig. 4.3, clearly indicates a substantial fall of around 1.7 MSm^3/day at the late production, while at some stages it is levelled the same as in the initial production. The reason could be that the variation in the constraint of the wellhead pressure. The dashed brown line indicate the cumulative gas production (Fig. 4.3). The gas production rate is kept constant and fixed when the Medium and Rich GC are used.

Fig. 4.3 also shows that Tg303bis well is historymatched and the good agreement is obtained between the measured well tubing-head pressure (THP) and the simulated THP of all WD approaches. The comparison of THP of WD approaches are also shown in Fig. B.1.1 and Fig. B.2.1 (Appendix B.1 and B.2) for Medium and Rich GC. For instance: in Lean GC, as the THP is dropped to about 140 bara in February 2007, the surface gas production slightly goes up before falling again after two months. Furthermore, it is also seen in the production and THP profiles, the well was shut in twice in June 2007 and in late 2010. After the former shut-in period the THP is not recovered so much.

Fig. 4.4, Fig. B.1.5 and Fig. B.2.5 (Appendix B.1 and B.2) represent the cumulative oil rate in dashed lines. In Lean GC and Rich GC there is no big difference in the cumulative oil rate after 5 years production between all of WD approaches, but the difference in seeen in Medium GC. For example: in Medium GC, the cumulative oil rate of WPI Mult approach is somewhat higher than the cumulative oil rate of Perm Mult appraoch which is in turn higher than in Fault Mult approach.

The above curves also depict the oil production rate of WD approaches in solid lines. For example: in Lean GC, the oil production of three WD approaches is peaked of around 680 Sm^3/day in late 2006 before dropping to 500 Sm^3/day. It is reached the peak again, but there is a substantial reduction in April 2007 which coincides with the gas production decrease at the same period (Fig. 4.4).

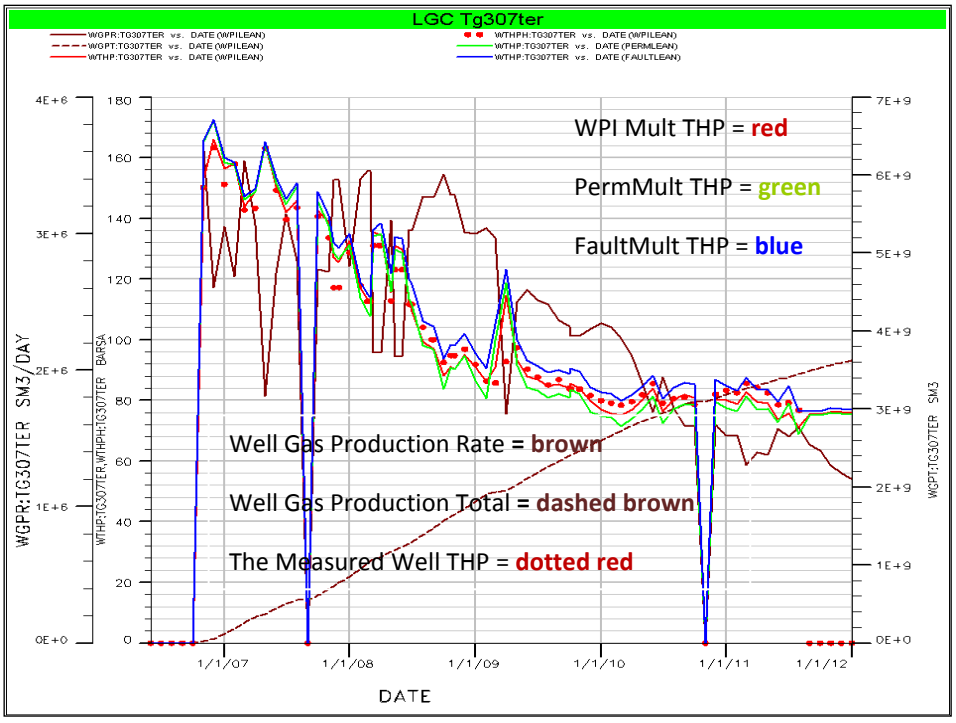

Fig. 4.2: The Tg307ter well historymatching of WD approaches, LGC

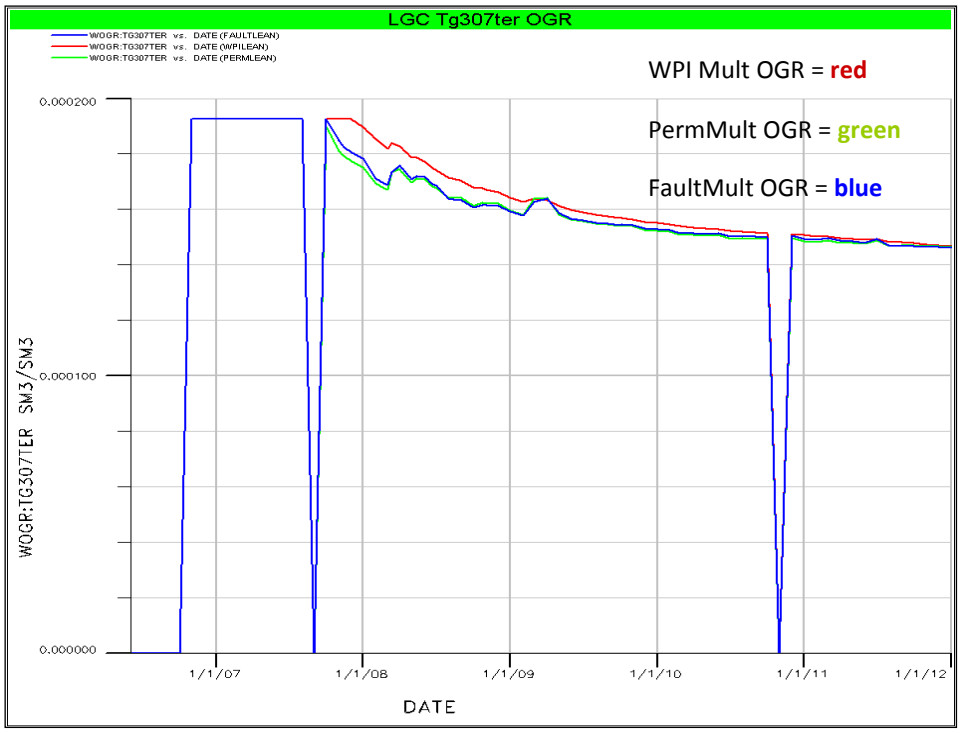

Fig. 4.3: The flowing OGR profile of WD approaches, Tg307ter, LGC

The well flowing OGR has undergone a considerable reduction as the reservoir is depleted (Fig. 4.3, Fig. B.1.2 and Fig. B.2.2). The curve also shows when the dewpoint pressure is reached for different WD approaches. It is believed that the flowing gas-oil ratio (GOR) is constant throughout Region 1 which means that the produced wellstream mixture is the same as the flowing composition of a single-phase gas entering Region 1. The dewpoint pressure of gas entering Region 1 is considered as the reservoir pressure at the outer edge of Region 1, p^*. In Lean GC, in WPI Mult approach the dewpoint pressure of the reservoir Region 1 is extended for 2.5 month compared to Perm Mult and Fault Mult approach. According to the Fig. B.1.2 and Fig. B.2.2, in Medium and Rich GC, the dewpoint pressure is reached as soon as the initial production is commenced.

In Lean, Medium and Rich GC, the well flowing OGRs indicate the various behavior between WD approaches as the dewpoint pressure is reached and the pressure falls below the dewpoint pressure. For example: Fig. 4.3 shows that the stable OGR above the dewpoint pressure is substantially decreased until late 2011 in WPI Mult approach as well as in Perm Mult and Fault Mult approaches. Moreover, all of three curves are overlaying on top each other from late 2011 to late 2012.

It is basically explained by the solution OGR of the well and neigbourhood grids depending on pressure depletion strategy. Fig. 4.7 shows that a grid solution OGR in the region around the well or Region 1 is extended from the well to around 100 m distance and it is constant throughout Region 1 in late 2007. It is observed in different fluid systems. After 5 years of production the size of Region 1 is around 400 m in Rich GC and about 300 m in Medium GC and about 200 m in Lean GC (Fig. 4.8).

It is believed that the size of Region 1 expands being the minimum size as the pressure in the vicinity of the well is just below the dewpoint pressure of gas entering Region 1. According to Fig. 4.9 and Fig. 4.10, in late 2007 and in late 2011 the well grid-cell and neighbouring grid-cells pressure is gradually reduced compared to initial pressure and in late 2011 is remained stable over 400 m distance in WPI Mult approach for different fluid systems, while in Perm Mult and Fault Mult approaches the grid-cell pressure is even dropped at the same distance range.

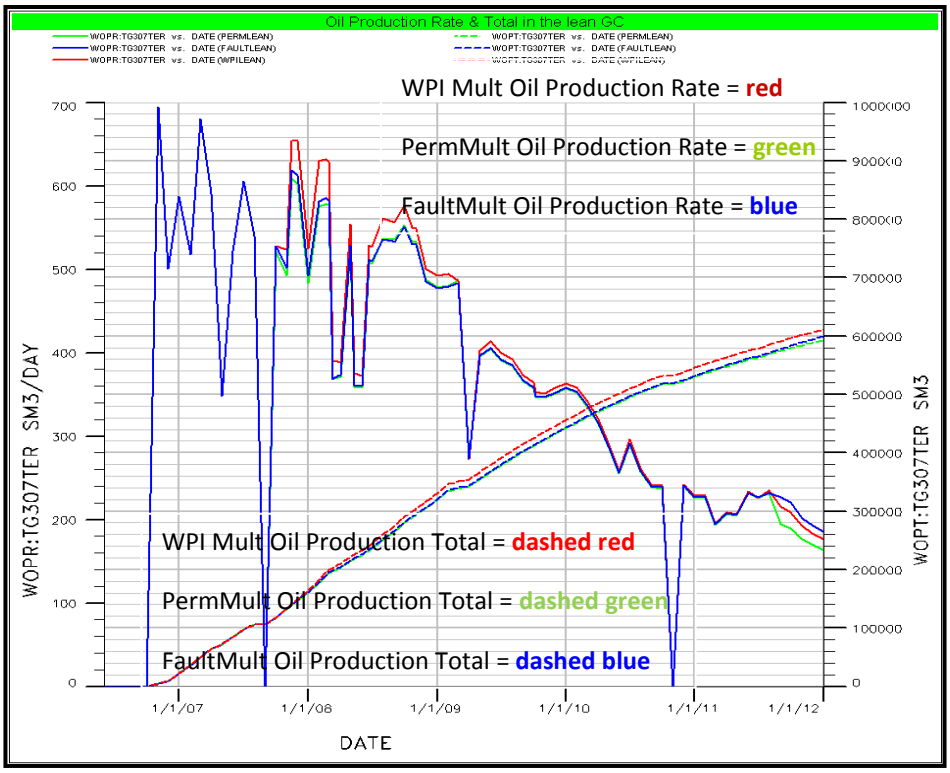

Fig. 4.4: The oil production rate and total of WD approaches vs. time, Tg307ter, LGC

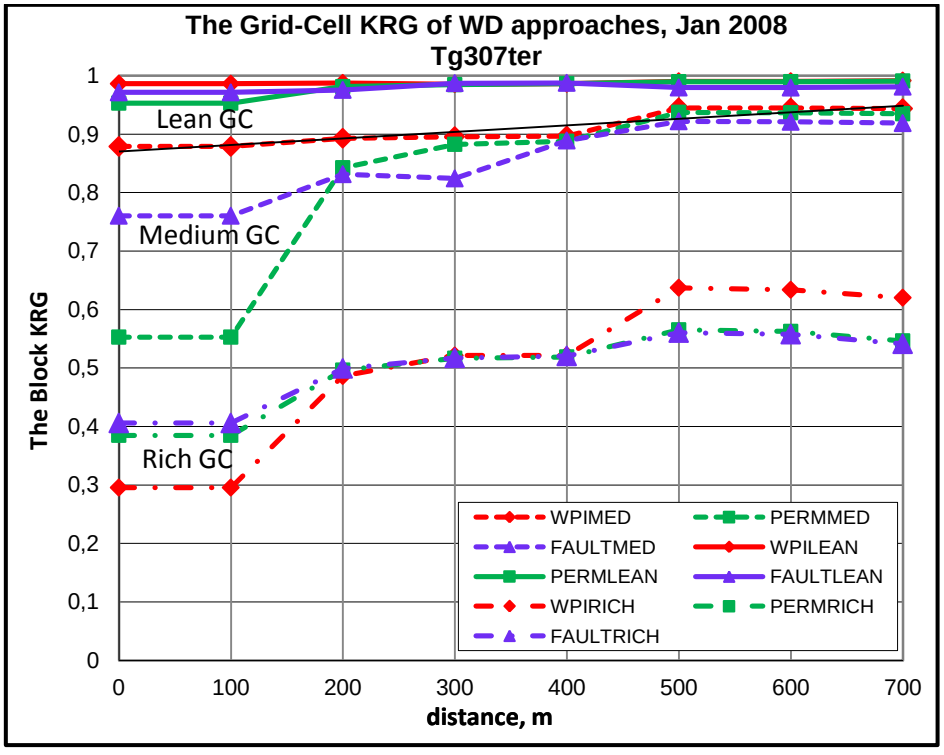

Fig. 4.5: The grid KRG of WD approaches vs. distance by Jan 2008, Tg307ter (1 case)

The difference in the well grid-cell pressure between WD approaches leads to formation of the different well grid-cell solution OGR. Therefore, after 5 years of production the well grid solution OGR of WD approaches becomes the same as the well flowing OGR, as discussed above. According to Fig. 4.9 and Fig. 4.10, it is somewhat difficult to justify the above distance range and the pressure at the outer edge of Region 1, p^* among different WD approaches.

According to Fig. 4.13, Fig. B.1.3 and Fig. B.2.3 (Appendix B.1 and B.2), there is a good agreement between the input solution OGR and the well grid solution OGR. If the well flowing OGRs of WD approaches are overlaying on top each other, it is because of the well grid solution OGRs of WD approcahes are also overlaying on top each other (Fig. B.2.2 and Fig. B.2.3). If the difference in the well flowing OGRs between WD approaches is observed, it is because of the difference in the well grid solution OGRs (Fig. B.1.2 and Fig. B.1.3).

As shown in the Fig. 4.5 and Fig. 4.6, the overall behavior of the grid gas relative permeability over the selected distance for Lean, Medium and Rich GC. For example: in Lean GC, in Jan 2008 there is a little reduction in the grid gas relative permeability, while it is slightly dropped in well grid in August 2011 by almost 7% and 4.3% in WPI Mult – Fault Mult approaches and Perm Mult approach respectively. The reason is that the gas relative permeability in Region 1 is mainly a function of liquid saturation distribution (Fevang et al., 1995).

All of three WD approaches have undergone a reduction in gas relative permeability in different degree, mostly the highest drop in well grid cell is seen in Fault Mult approach in both Lean and Medium GC. However, as the steady-state liquid saturation is reached in Rich GC, the gas relative permeability of three WD approaches is slightly increased after 5 years of production from the well grid to 400 m distance. As it is mentioned above, the drop in liquid saturation can be observable only after a period of production time when a steady-state is reached. The main reason of reduction in liquid saturation is the composition of a single-phase phase entering Region 1 which will become leaner and leaner dropping out more heavy components. The relative permeability and liquid saturation are a function of time and the pressure drawdown in Region 1 which depends on the PVT and fluid properties of a single-phase gas leaving Region 2 (Fevang et al., 1995).

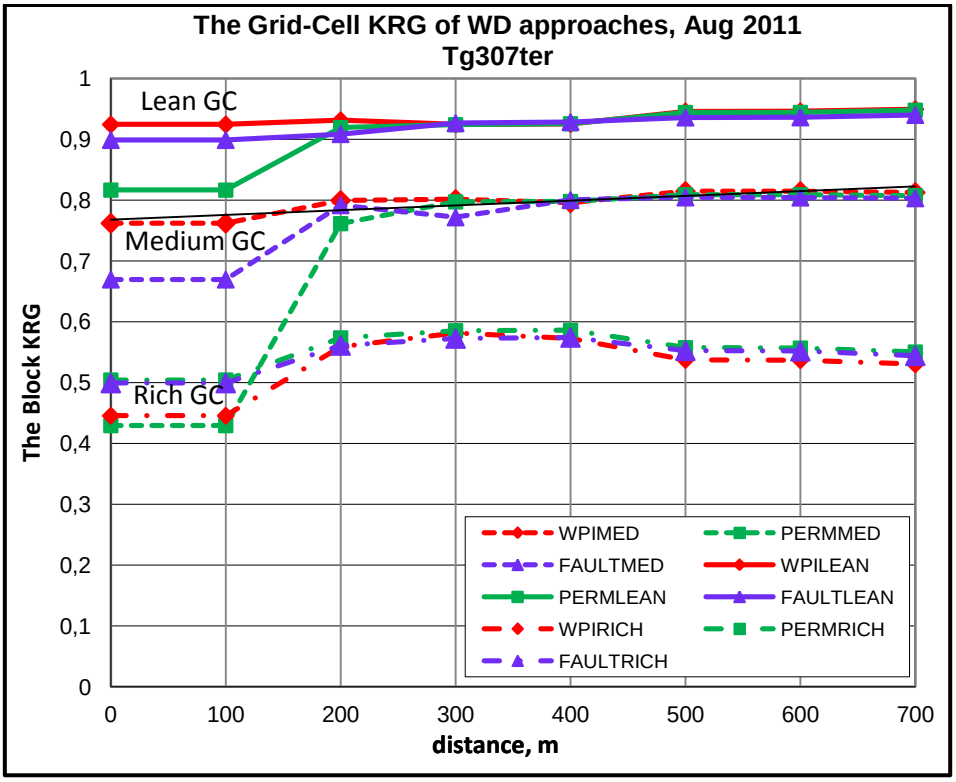

Fig. 4.6: The grid KRG of WD approaches vs. distance by Aug 2011, Tg307ter (1 case)

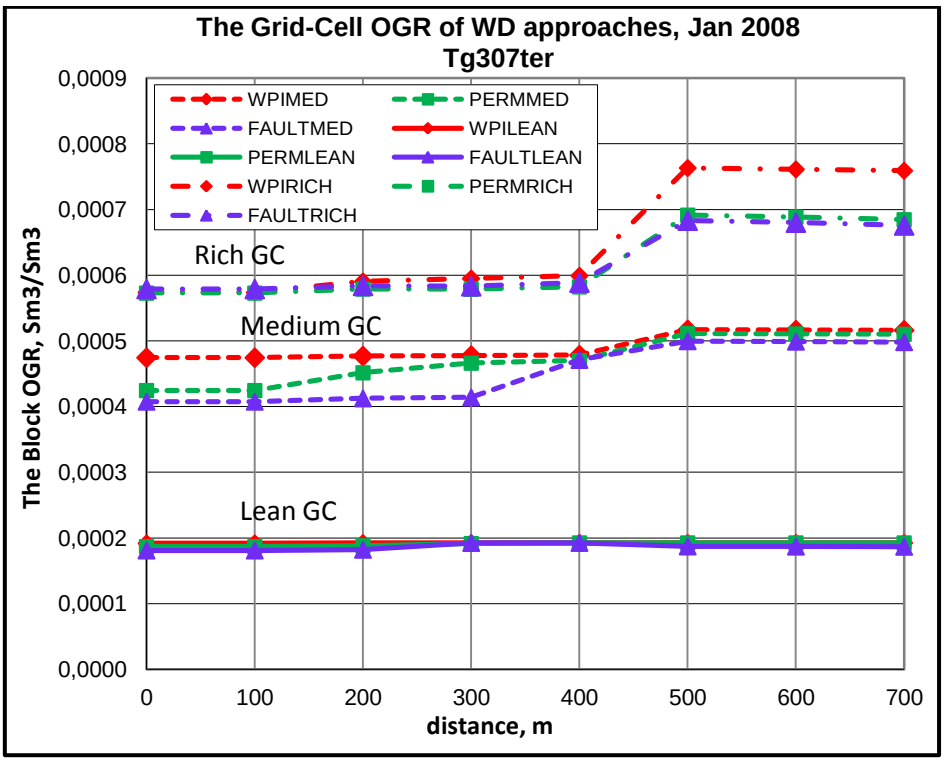

Fig. 4.7: The grid OGR of WD approaches vs. distance by Jan 2008, Tg307ter (1 case)

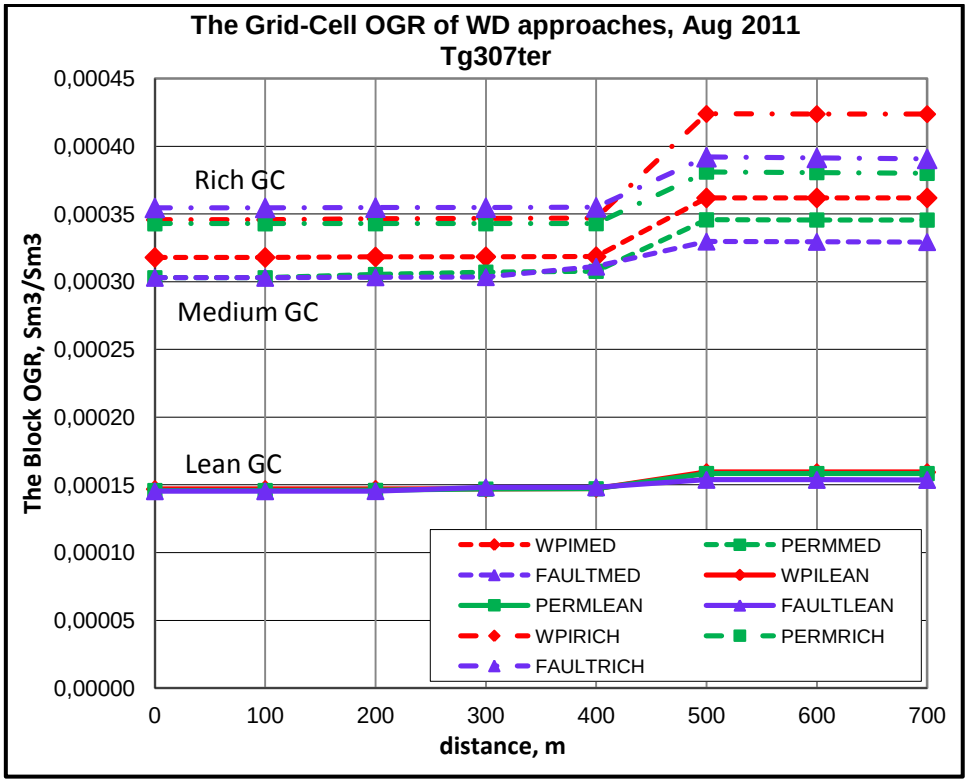

Fig. 4.8: The grid OGR of WD approaches vs. distance by Aug 2011, Tg307ter (1 case)

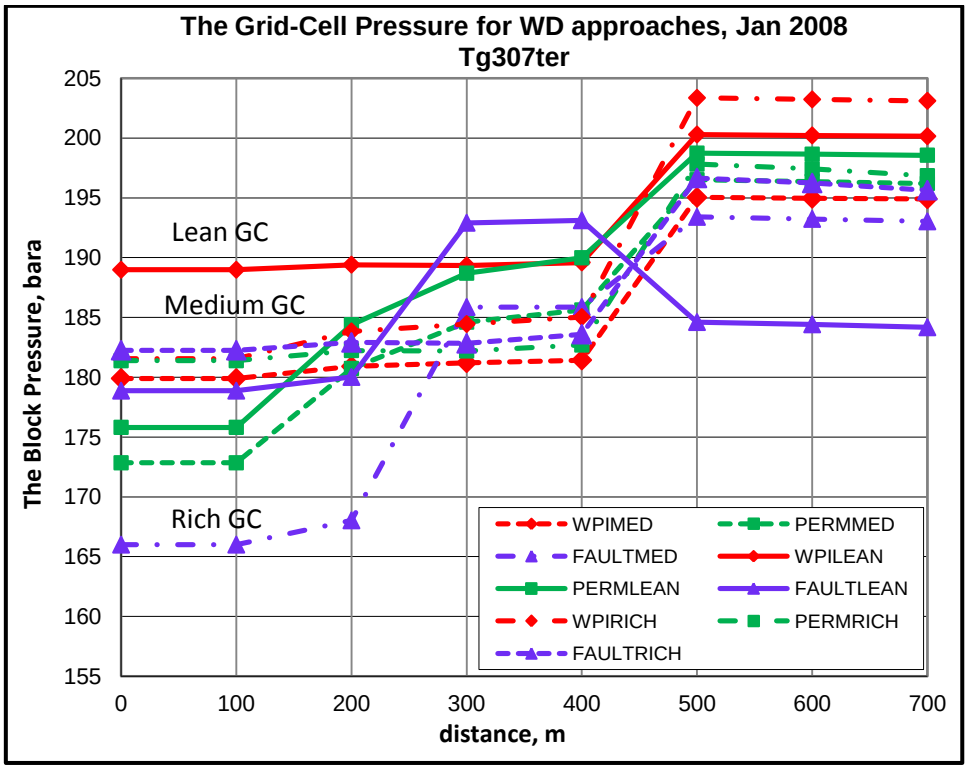

Fig. 4.9: The grid Pressure of WD approaches vs. distance by Jan 2008, Tg307ter (1 case)

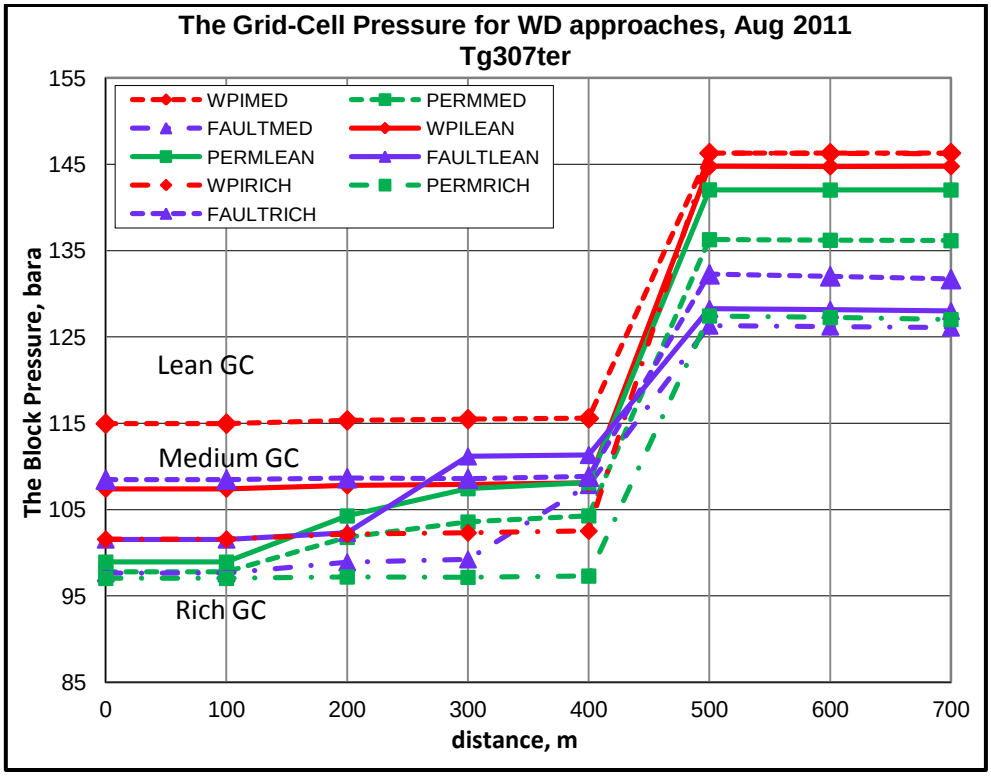

Fig. 4.10: The grid Pressure of WD approaches vs. distance by Aug 2011, Tg307ter (1 case)

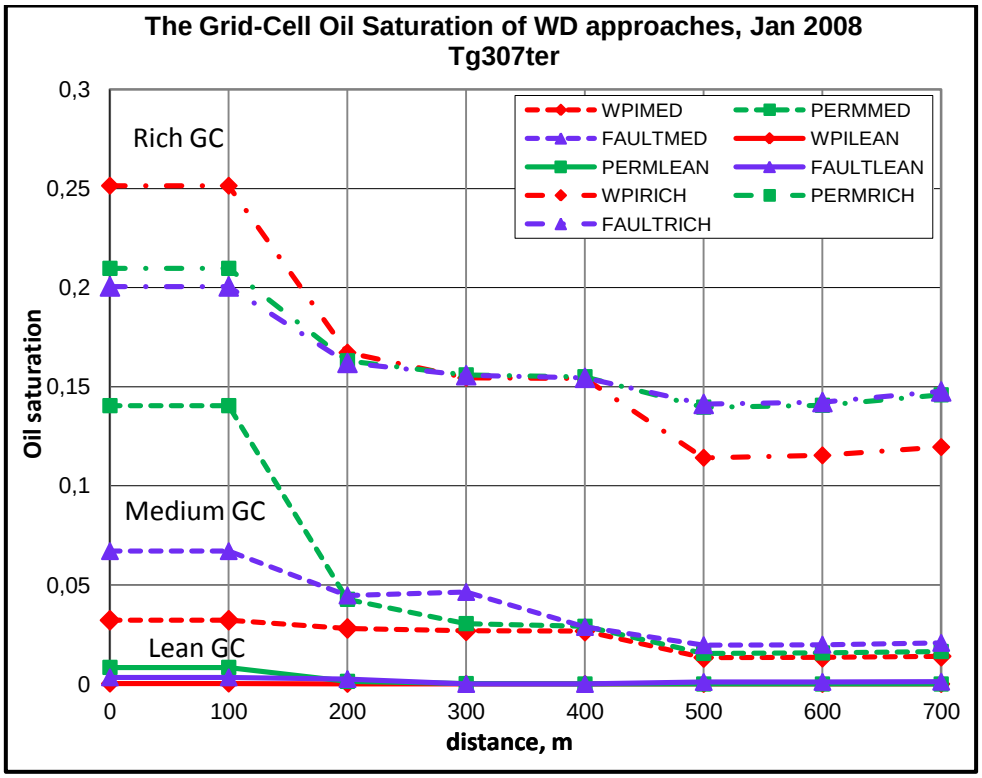

Fig. 4.11: Oil saturation of WD approaches vs. distance by Jan 2008, Tg307ter (1 case)

Furthermore, based on the oil saturation throughout the selected distance shown in Fig. 4.11 and Fig. 4.12, one can predict the appearence of steady-state saturation distribution. According to Fig. 2.4, the mobile condensate starts flowing in Region 1 after a short transition period and the size of Region 1 gradually expands outwardly, but there is a little reduction in the liquid saturation after 10 years of production. The reason is that gas leaving Region 2 becomes leaner.

The same behavior of liquid saturation is seen in Fig. 4.12 in Rich GC, which is consireably increased since the initial production has started, but in late 2011 the small reduction in liquid saturation is occurred in Region 1. In addition, one can also observe the outward expansion of the size of Region 1. It means that the steady-state liquid saturation is reached at that moment. However, the growth of liquid saturation still happens in Lean and Medium GC after 5 years of production and the steady-state saturation has not reached yet. For example: in Lean GC it is observed that, in January 2012 there are moderate rise in the grid oil saturation of three WD approaches compared to January 2008. The line charts depict that the grid oil saturation is increased towards the well grid cell and the highest increase in the well grid cell is seen in the Perm Mult approach (Fig. 4.11 and Fig. 4.12). The rapid depletion of reservoir in Rich GC leads to reaching the reservoir outer boundaries and the setting of steady-state flow.

The appearance of the steady-state liquid saturation in Rich GC is observed among all of three WD approaches. The continuous growth in liquid saturation is seen in WPI Mult, Perm Mult and Fault Mult approches after 5 years of production in Lean GC and Medium GC (Fig. 4.11 and Fig. 4.12).

Fig. 4.14 shows normalized input oil and gas relative permeability as a function of gas saturation and unnormalized gas relative permeability of the well grid cell for Case 1, Case 2 and Case 3 in all of three WD approaches. In Lean GC, in Case 1 gas relative permeability is gradually decreased in WPI Mult, Perm Mult and Fault Mult approaches after 5 years of production as the gas saturation is dropped when the pressure is below the dewpoint pressure of gas entering Region 1. In Case 2 and Case 3 gas relative permeabiltiy is almost remained the same as in Case 1, but gas saturation is even reduced in Case 2 and it is somewhat increased in Case 3. In numerical study of Case 2 and Case 3 shows that the

distribution of grid solution OGR and grid pressures almost matches Case 1 over the same distance range. Change in gas relative permeability and saturation is also observed in Medium and Rich GC, as shown in Fig. B.1.4 and Fig. B.2.4 (Appendix B.1 and B.2).

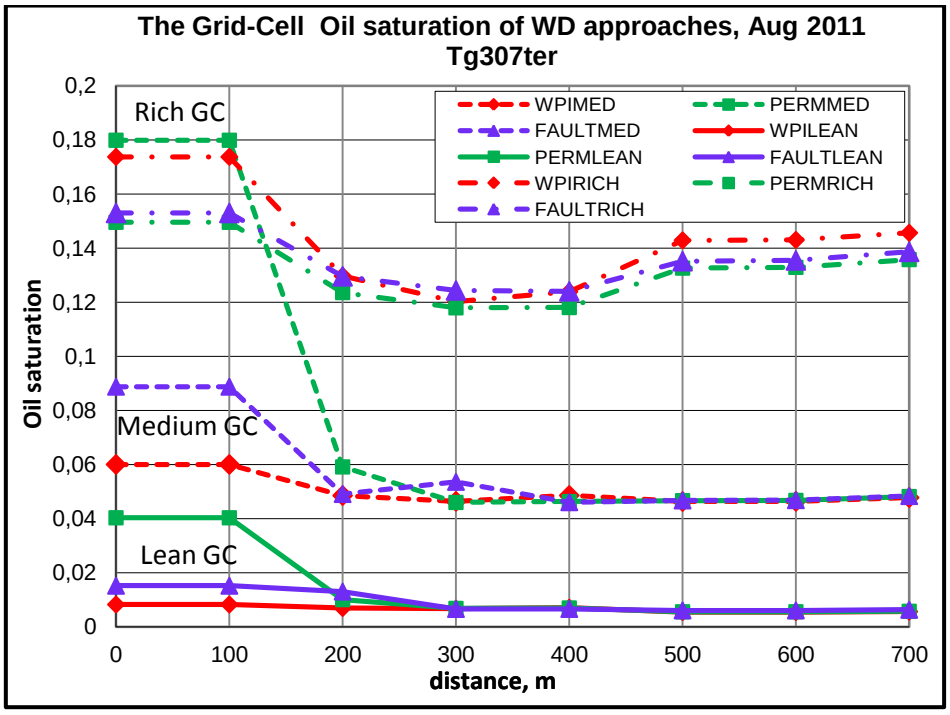

Fig. 4.12: Oil Saturation of WD approaches vs. distance by Aug 2011, Tg307ter (1 case)

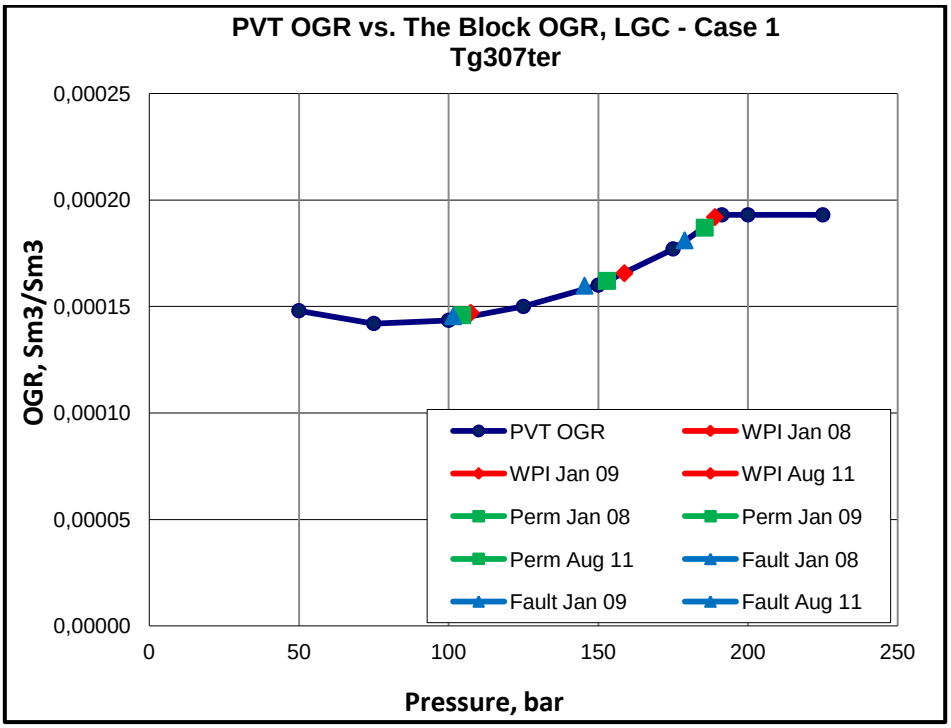

Fig. 4.13: The input PVT OGR and the well grid OGR vs. pressure, Tg307ter, LGC

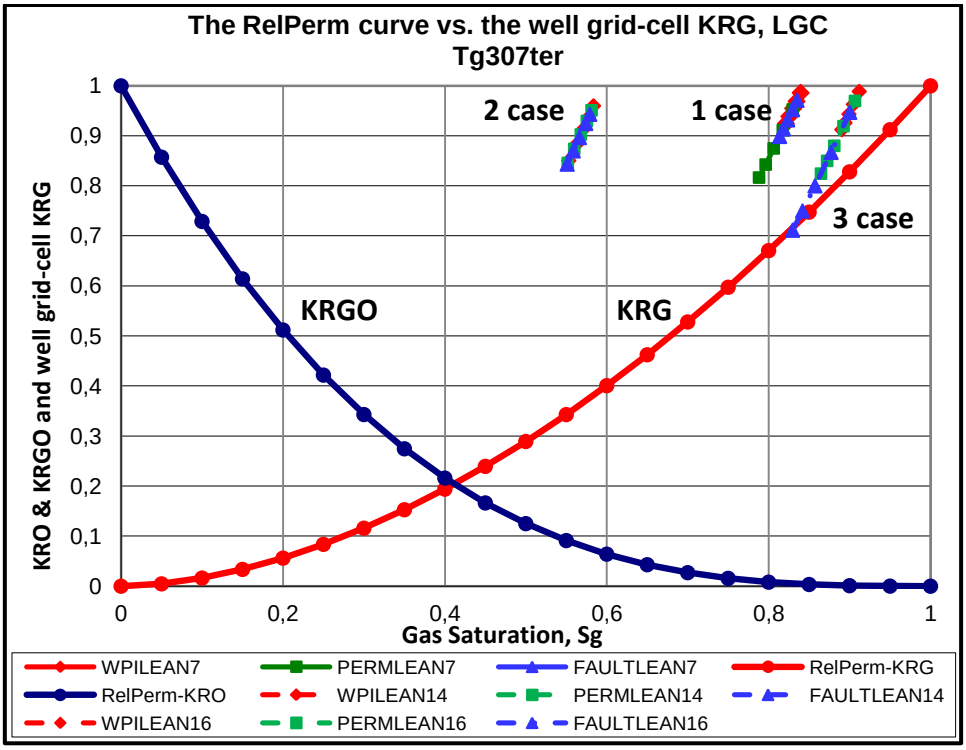

Fig. 4.14: The input RelPerm curve and the well grid RelPerm vs. pressure, Tg307ter, LGC

4.4.2. Tg303bis simulation result

Let us now look at the second well Tg303bis which is selected to fulfill an objective of numerical simulation study and confirm the importance of Region 1. Numerical simulation study is conducted by original Lean, fictitious Medium and Rich gas-condensate reservoirs.

Fig. 4.15 shows that Tg303bis well is historymatched and the good agreement is obtained between the measured well tubing-head pressure (THP) and the simulated THP of all WD approaches. In addition, in Lean GC the surface gas production of Tg303bis well is commenced in late 2007 and it is peaked of around 2.6 MM Sm^3/day after one year of production, shown as solid brown line and the dotted brown curve illustrates the cumulative gas production. The increased gas production at surface could be accomplished by reducing the tubing head pressure (THP) to the value of 130 bara and then it could be even lowered to maintain the initial rate. Unfortunately, as the THP is further dropped to 90 bara in middle 2009, the surface gas production is not able to maintain the previous initial rate because the outer pressure of Region 1 is already below the dewpoint pressure.

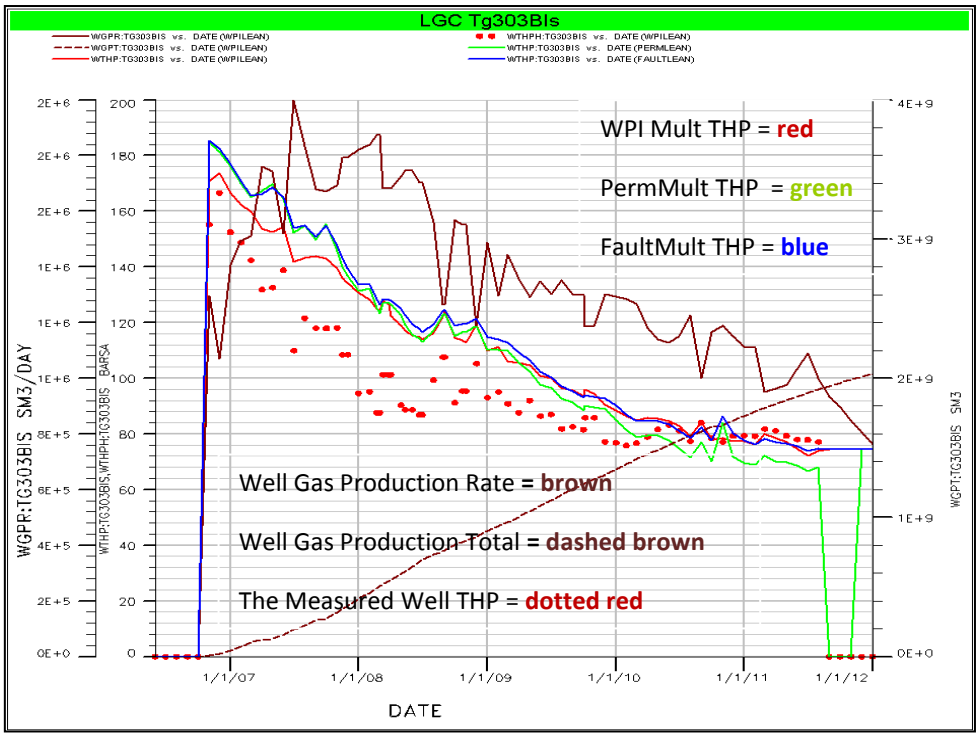

Fig. 4.15: The Tg303bis well historymatching of WD approaches, LGC

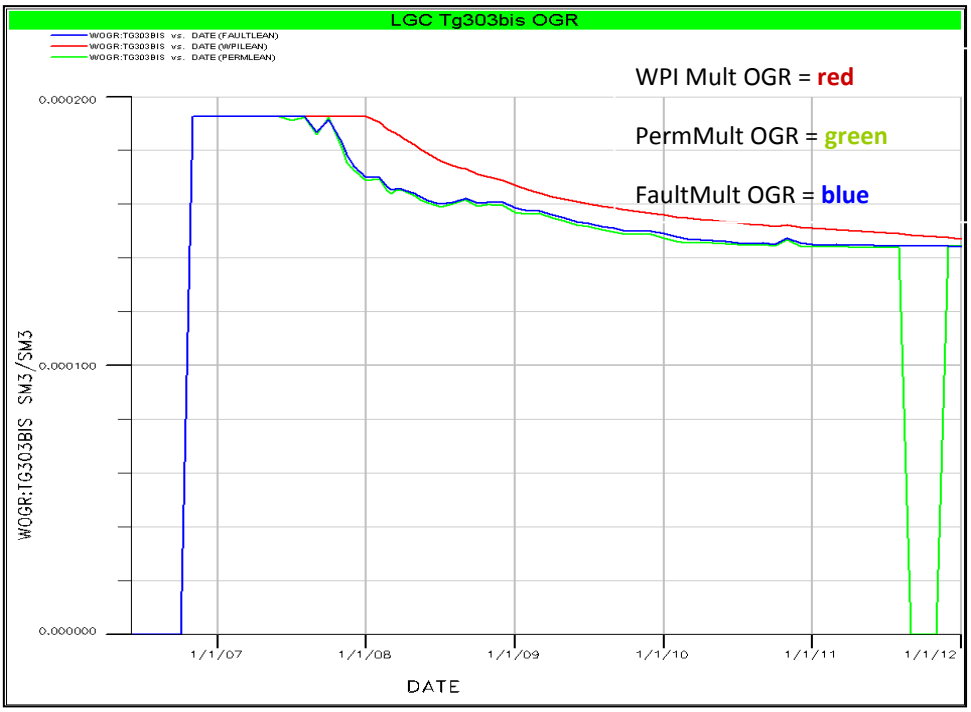

Fig. 4.16: The flowing OGR profile of WD approaches, Tg303bis, LGC

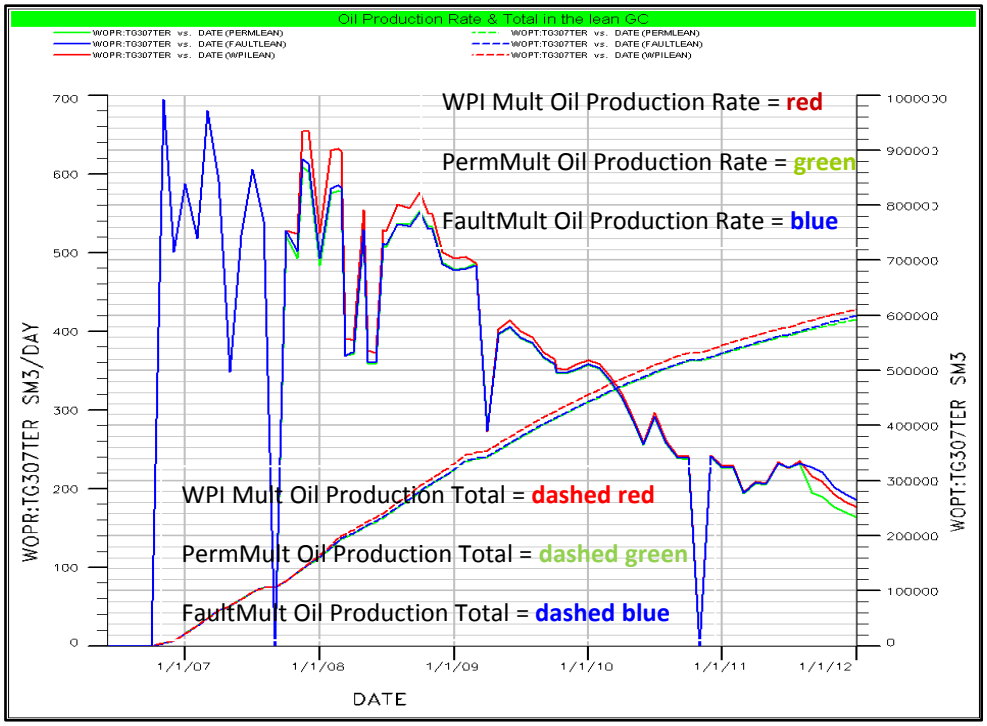

Fig. 4.17: The oil production rate and total of WD approaches vs. time, Tg303bis, LGC

Furthermore, the pressure is gradually lowered until the beginning of 2009 and it is stabilized because of pressure support from the surrounded aquifer (Fig. 4.16). The gas production rate is kept constant and fixed when the Medium and Rich GC are used.

Fig. C.1.1 and Fig. C.2.1 (Appendix C.1 and C.2) also represent the comparion of THP of WD approaches for Medium and Rich GC. In overall, in Medium GC the comparison of THP between WD approaches is reasonbly made. As shown in Fig. C.2.1, in rich GC the reasonable comparison of THP is not accomplished after about 2 years of production, but in last 3 years of production it is almost overlaying on top each other (Fig. C.2.1). Therefore, the substantial separation in THPs between WD approaches in Rich GC could lead to the different flowing OGR response.

Fig. 4.17, Fig. C.1.2 and Fig. C.2.2 represent the cumulative oil rate in dashed lines. The difference in the cumulative oil rate in seen in Medium GC between all of WD approaches, but in Lean GC and Rich GC there is no big difference in the cumulative oil rate after 5 years production. The above curves also depict the oil production rate of WD approaches in solid lines. For example: Fig. 4.17 depicts that oil production rate at surface is considerably increased and reached a peak of around 650 Sm^3/day in all three WD approaches.

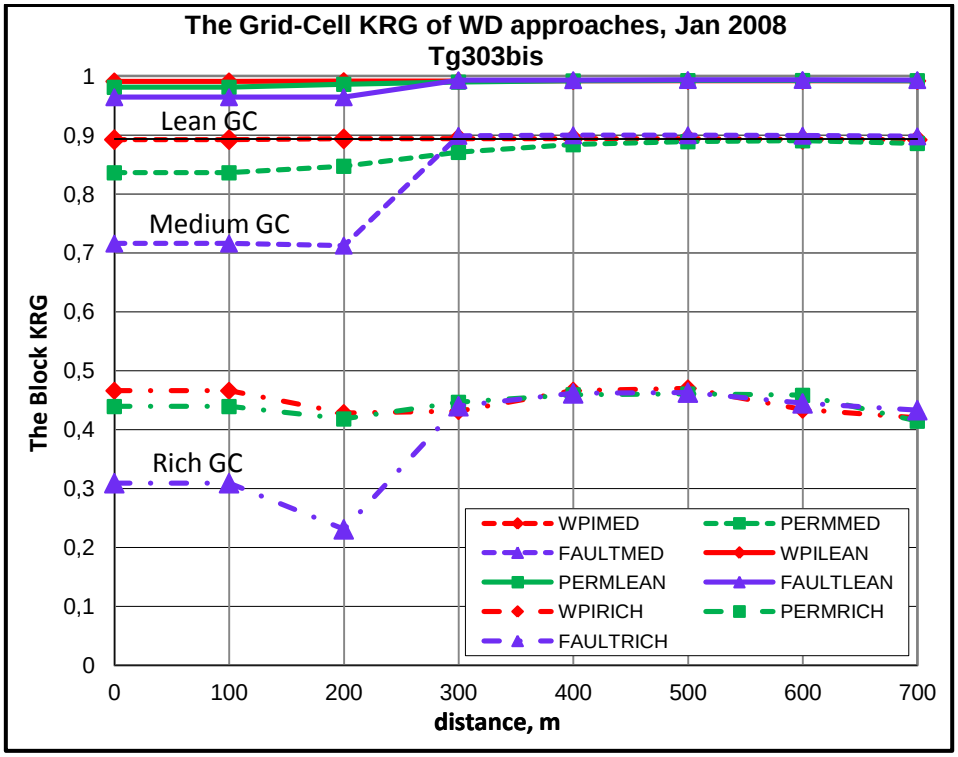

Fig. 4.18: The grid KRG of WD approaches vs. distance by Jan 2008, Tg303bis (1 case)

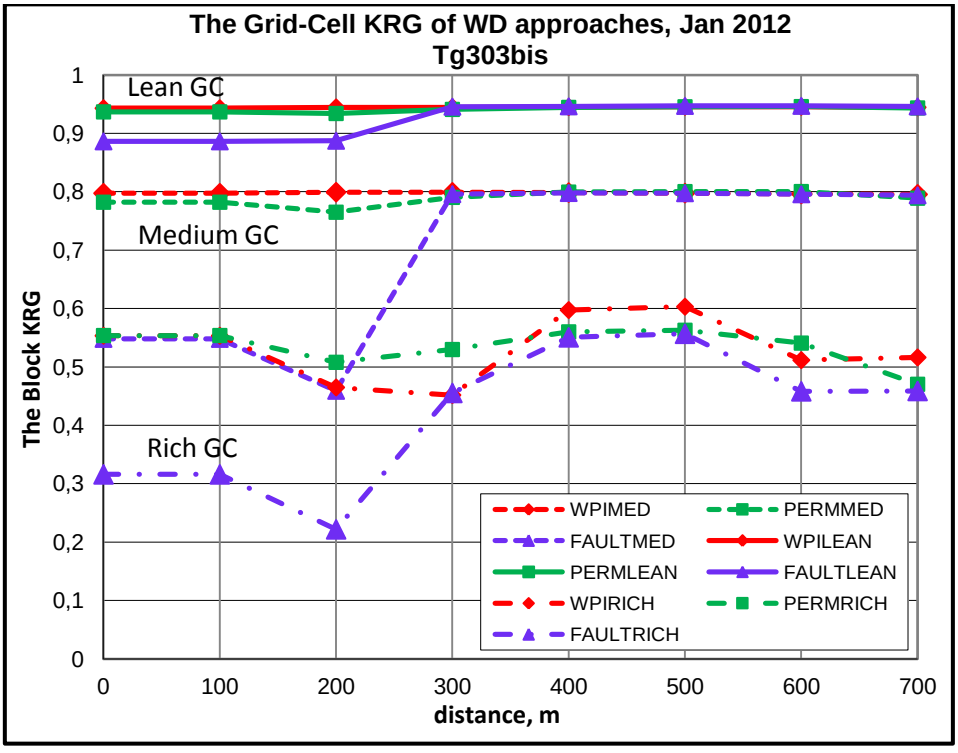

Fig. 4.19: The grid KRG of WD approaches vs. distance by Jan 2012, Tg303bis (1 case)

The well flowing OGR has undergone a considerable reduction as the reservoir is depleted (Fig. 4.16, Fig. C.1.3 and Fig. C.2.3). The curve shows when the dewpoint pressure is reached for different WD approaches. As mentioned above, it is believed that the flowing gas-oil ratio (GOR) is constant throughout Region 1 which means that the produced wellstream mixture is the same as the flowing composition of a single-phase gas entering Region 1. The dewpoint pressure of gas entering Region 1 is considered as the reservoir pressure at the outer edge of Region 1, p^*.

Fig. 4.16 depicts that the initial dewpoint of the reservoir is reached in middle 2008 for Perm Mult and Fault Mult approaches, whereas it is extended for almost 3 months for WPI Mult approach. The reduction in the surface gas production coincides with the appearance of the initial dewpoint pressure. In addition, Fig. C.1.3 shows that the difference in the flowing OGRs between three WD approaches is remained until the middle 2012, while it is almost vanished between Perm Mult and Fault Mult approaches in the late production period.

It is basically explained by the solution OGR of the well and neigbourhood grids. Fig. 4.20 shows that a grid solution OGR in Region 1 is remained the same between the well and 100 m distance in late 2007 in all of fluid systems. Fig. 4.21 depicts that in late 2011 the size of Region 1 is gradually increased such that it is about 600 m in Lean, Medium and Rich GC.

As also mentioned above, it is believed that the size of Region 1 increases gradually being the minimum size as the pressure in the vicinity of the well is just below the dewpoint pressure of gas entering Region 1. The size of Region 1 gradullay expands with time and pressure depletion strategy.

According to Fig. 4.22 and Fig. 4.23, in late 2007 and in late 2011 the grid cell pressure is gradually decreased compared to initial production case and is levelled off over the selected distance in WPI Mult approach for different fluid systems, while in Perm Mult and Fault Mult approaches the grid-cell pressure is distributed differently and the highest drop is remained in the well grid-cell. The difference in the well grid-cell pressure leads to formation of different well grid-cell solution OGR. Therefore, as the reservoir is depleted after 5 years of production the well grid-cell OGR of WD approaches becomes the same, as discussed above.

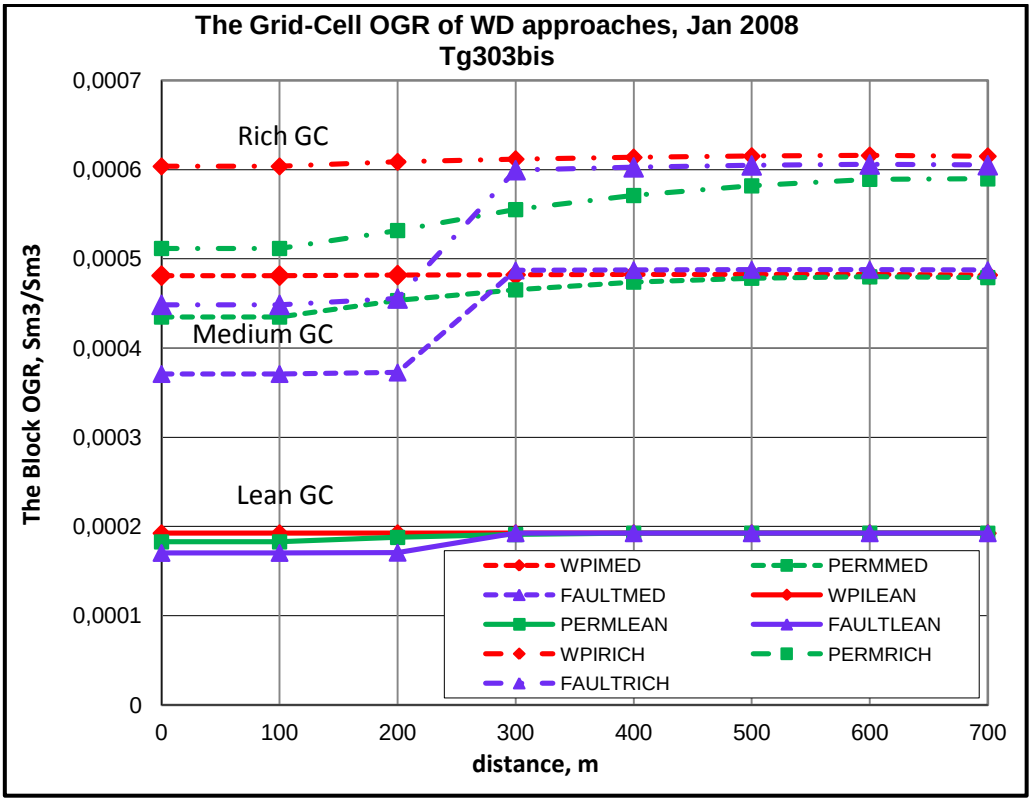

Fig. 4.20: The grid OGR of WD approaches vs. distance by Jan 2008, Tg303bis (1 case)

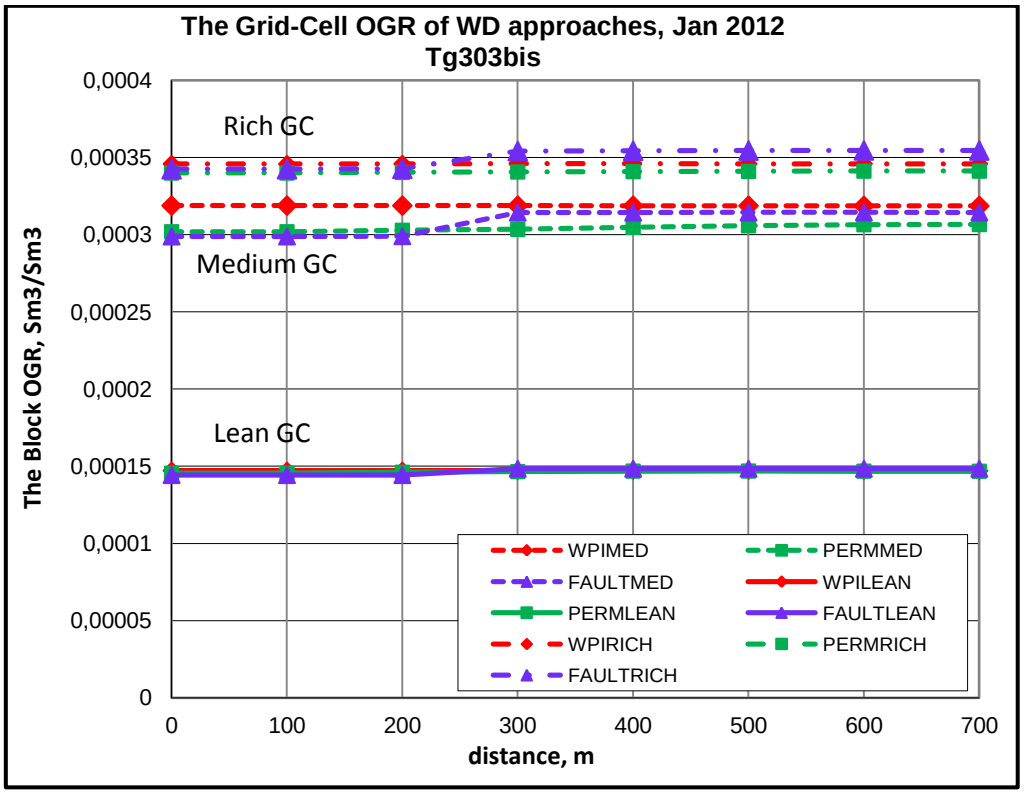

Fig. 4.21: The grid OGR of WD approaches vs. distance by Jan 2012, Tg303bis (1 case)

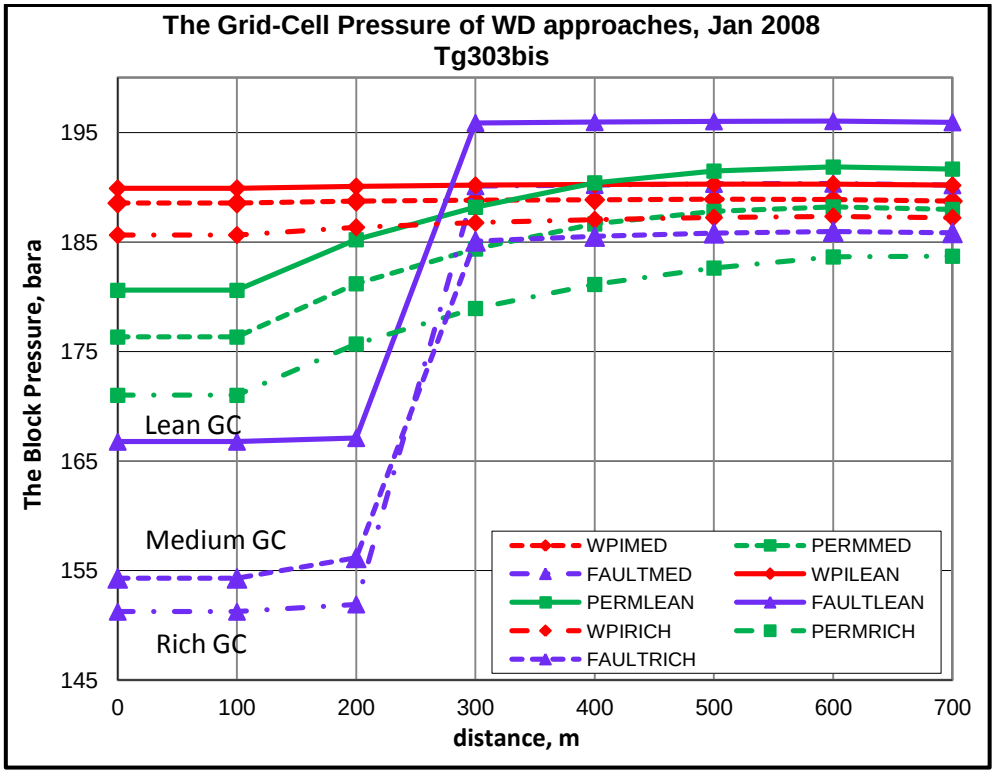

Fig. 4.22: The grid Pressure of WD approaches vs. distance by Jan 2008, Tg303bis (1 case)

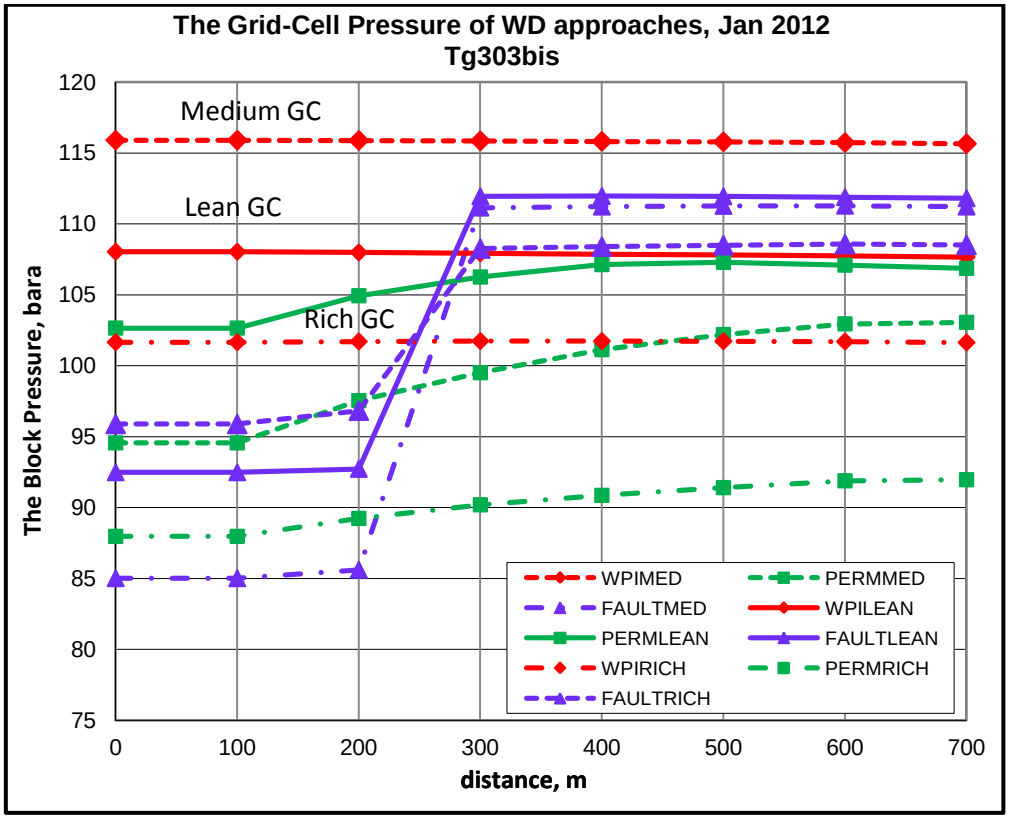

Fig. 4.23: The grid Pressure of WD approaches vs. distance by Jan 2012, Tg303bis (1 case)

Fig. 4.26, Fig. C.1.4 and Fig. C.2.4 (Appendix C.1 and C.2), there is a good agreement between the input solution OGR and the well grid solution OGR. If the well flowing OGRs of WD approaches are overlaying on top each other, it is because of the well grid solution OGRs of WD approcahes are also overlaying on top each other (Fig. 4.16 and Fig. 4.26). If the difference in the well flowing OGRs between WD approaches is observed, it is because of the difference in the well grid solution OGRs (Fig. C.1.3 and Fig. C.1.4).

As shown in the Fig. 4.18 and Fig. 4.19, the overall behavior of the grid gas relative permeability over the selected distance for Lean, Medium and Rich GC. For example: In Lean GC the grid gas relative permeability is reduced in all three approaches over the entire distance, but it is insignificant and close to 1.0 after 1.3 year of production. However, it is further dropped in late 2011 and it is still not so dramatic change.

All of three WD approaches have undergone a reduction in grid-cell gas relative permeability in different degree, mostly the highest drop in well grid cell is seen in Fault Mult approach in both Lean and Medium GC. However, as the steady-state liquid saturation is reached and the size of Region 1 is gradually increased outwardly in Rich GC, after 5 years of production the grid-cell gas relative permeability of three WD approaches is slightly increased. The reason it that the gas relative permeability in Region 1 is mainly a function of liquid saturation distribution (Fevang et al., 1995).

Fig. 4.25 shows the appearence of steady-state liquid saturation in Rich GC. The liquid saturation is gradually increased since the initial production has started. However, in late 2011 the small reduction in liquid saturation is occurred in Region 1. The steady-state liquid saturation is reached at that moment when the outward expansion of the size of Region 1 is observed. However, the growth of liquid saturation still happens in Lean and Medium GC after 5 years of production and the steady-state saturation has not reached yet. The rapid depletion of reservoir in Rich GC leads to reaching the reservoir outer boundaries and the setting of steady-state flow.

As it is mentioned above, the drop in liquid saturation can be observable only after a period of production time when a steady-state is reached. The main reason of reduction in liquid saturation is the composition of a single-phase phase entering Region 1 which will become leaner and leaner dropping out more heavy components.

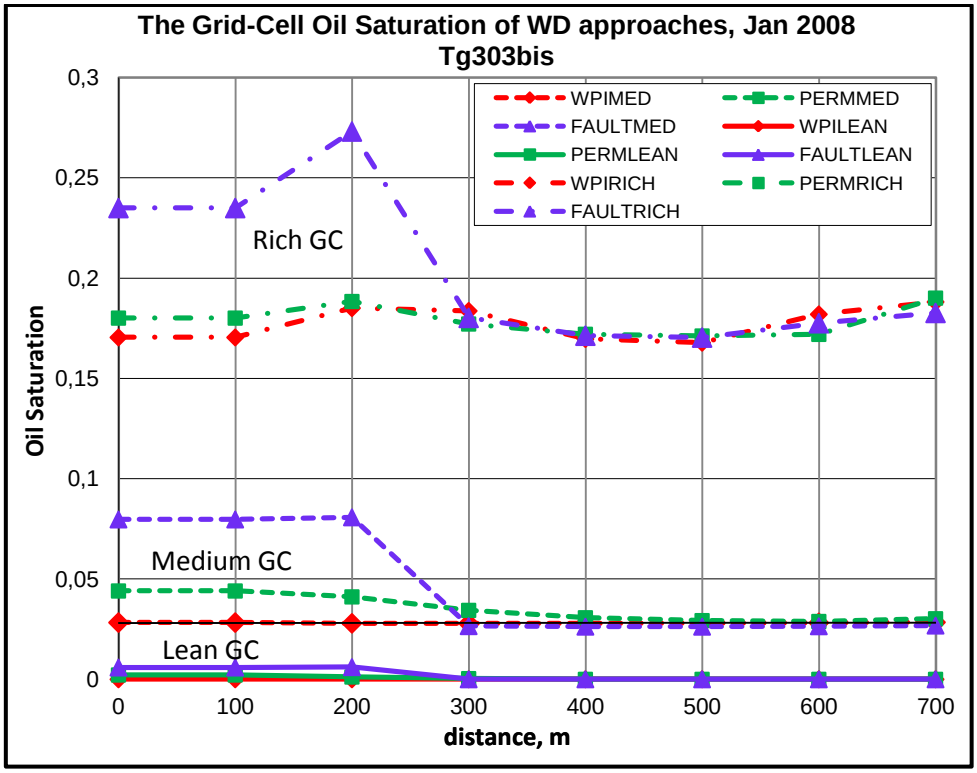

Fig. 4.24: Oil Saturation of WD approaches vs. distance by Jan 2008, Tg303bis (1 case)

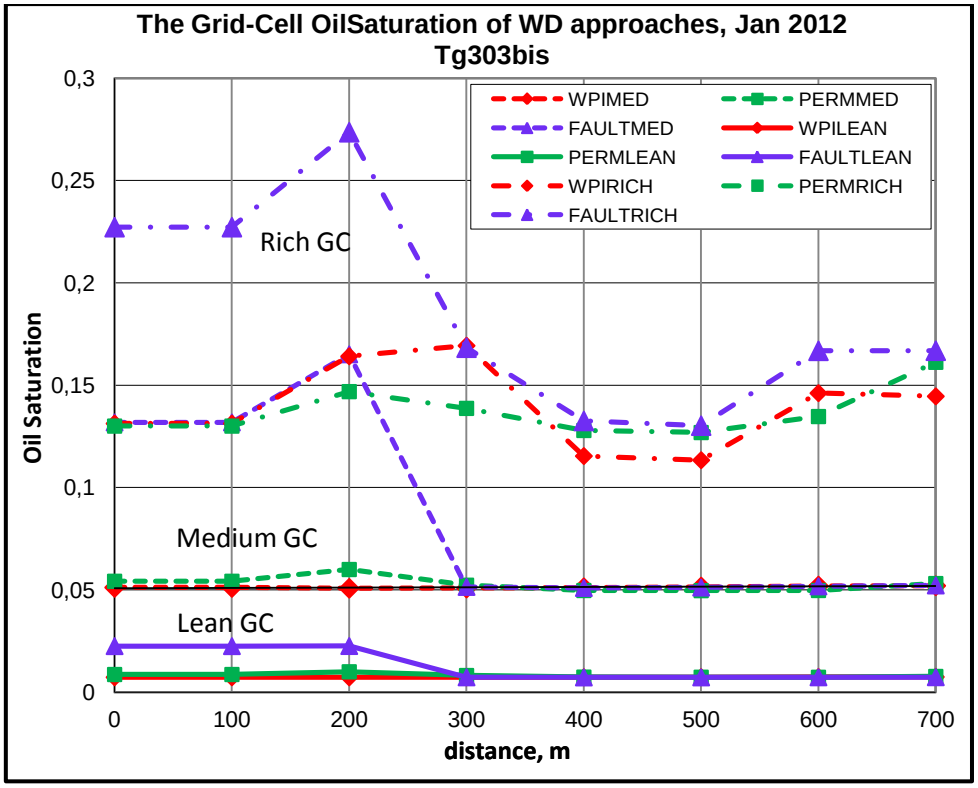

Fig. 4.25: Oil Saturation of WD approaches vs. distance by Jan 2012, Tg303bis (1 case)

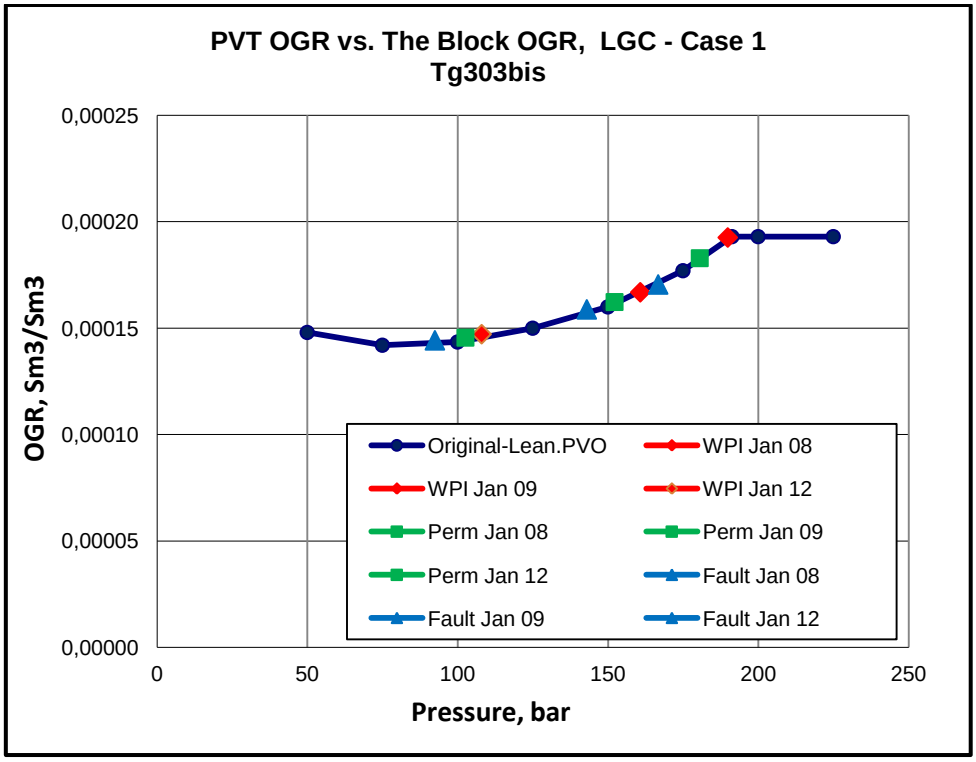

Fig. 4.26: The input PVT OGR and the well grid OGR vs. pressure, Tg303bis, LGC

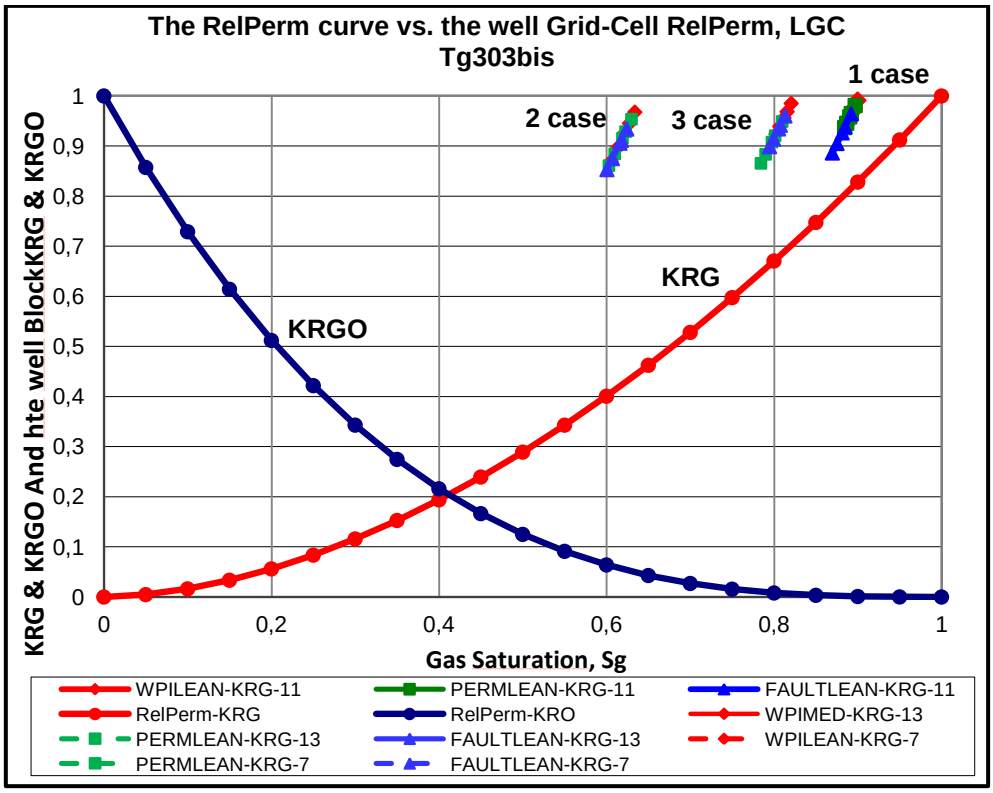

Fig. 4.27: The input RelPerm curve and the well grid RelPerm vs. pressure, Tg303bis, LGC

The appearance of the steady-state liquid saturation in Rich GC is observed among all of three WD approaches. The continuous growth in liquid saturation is seen in the WPI Mult, Perm Mult and Fault Mult approches after 5 years of production in Lean GC and Medium GC (Fig. 4.24 and Fig. 4.25). The relative permeability and liquid saturation are a function of time and the pressure drawdown in this region which depends on the PVT and fluid properties of a single-phase gas leaving Region 2 (Fevang et al., 1995).

Fig. 4.27 shows normalized input oil and gas relative permeability as a function of gas saturation and unnormalized gas relative permeability of the well grid cell for Case 1, Case 2 and Case 3 in all of three WD approaches. In numerical study of Case 1, Case 2 and Case 3 shows that the distribution of grid solution OGR and grid pressures is the similar to each other in the selected distance in late 2007 and late 2011. For example: in Lean GC, when the pressure is below the dewpoint pressure of gas entering Region 1, gas relative permeability in Case 1 is gradually decreased in WPI Mult, Perm Mult and Fault Mult approaches after 5 years of production as the gas saturation is dropped. In Case 2 and Case 3 gas relative permeabiltiy is remained the same as in Case 1, but gas saturation is even reduced in Case 2 and Case 3. Change in gas relative permeability and saturation is also observed in Medium and Rich GC, as shown in Fig. C.1.5 and Fig. C.2.5 (Appendix C.1 and C.2).

Chapter 5

Conclusions and Discussion

5.1. Conclusions

Numerical simulation studies are performed to quantify the impact of the historymatching, represented by three well deliverability approaches, on the flowing oil-gas ratio (OGR) in a coarse grid B-O model. Medium and Rich GC PVT and fluid properties are separately included in a B-O model, for a fictitious reservoir, while Lean GC is produced from the current actual field In Amenas field, Tiguentourine structure.

Alternative well deliverability approaches investigated are called "Perm Mult" and "Fault Mult" with adjustment of permeability or transmissibility of numerical blocks surrounding the well blocks. The region around the well is an important area for historymatching procedure in gas-condensate reservoirs. The Perm Mult and Fault Mult WD approaches can be used in the same degree as the WPI Mult approach in the historymatching procedure. The difference in the cumulative oil production between three WD approaches is noticeable in Medium GC, while it is almost overlaying on top each other in Lean GC and Rich GC.

The condensate impairment to the gas flow is well-known issue in gas-condensate fileds, but it is not accounted in a coarse-gridded model. The behavior of the important Region 1 and the change in the size of Region 1 are observed in well grid-cell and neigbouring grid cells. The steady-state liquid saturation is seen in Rich GC behavior after 5 years of production.

Our work has led to conclude that the historymatching of well deliverability approaches has an impact on the well flowing oil-gas ratio and it is proposed to consider alternative well deliverability approaches before starting to tune fluid properties in order to obtain a reasonable match between the measured oil-gas ratio and the simulated one.

5.2. Future work

The dependent of the relative permeabilities on capillary number effect is not considered in these numerical studies and it will be beneficial to observe the impact of the historymatching of three well deliverability approaches on the flowing OGRs in the vicinity of the well by compositional model with the lumped pseudo components.

References

1. Ahmed, H.E., Forrest, J.K., Fan, L., and McCain, W.D.: "*Producing Rich-Gas-Condensate Reservoirs—Case History and Comparison between Compositional and Modified Black-Oil Approaches" p*aper SPE 0000, 2000.
2. Al-Anazi, H.A., Okasha, T.M., Haas, M.D. and Ginest, N.H.: *"Impact of Completion Fluids on Productivity in Gas/Condensate Reservoirs*", *paper SPE 94256*, Oklahoma City, U.S.A., 2005.
3. Al-Anazi, H.A., Xiao, J.J., Al-Eidan, A.A., Buhidma, I.M., Ahmed, M.S., Al-Faifi, M.G. and Assiri, W.A.: *"Gas productivity Enhancement by Wettability Alteration of Gas-Condensate Reservoirs" paper SPE 107493*. Scheveningen, The Netherlands, 2007.
4. Al Ismail, M.I.: *"Field Observations of Gas-Condensate Well Testing", M.S. thesis (2010)*, CA., Stanford University.
5. Ayyalasomayajula, P., Silpngarmlers, N. and Kamath, J.: *"Well Deliverability Predictions for a Low-Permeability Gas/Condensate Reservoir" paper SPE 95529.* Texas, U.S.A., 2005.
6. Baig, T., Droegemueller, U. and Grindarten, A.C.: "*Productivity Assessment of Fractured and Non-fractured wells in a Lean/Intermediate Low Permeability Gas Condensate Reservoir" paper SPE 93136*. Madrid, Spain, 2005.
7. Barnum, R.S., Brinkman, F.P., Richardson, T.W. and Spillette A.G.: *"Gas Condensate Reservoir Behavior: Productivity and Recovery Reduction Due to Condensation" paper SPE 30767.* Dallas, U.S.A., 1995.
8. Blom, S.M.P., Hagoort, J., Soetekouw, D.P.N.: *"Relative Permeability at Near-Critical Conditions", paper SPE 38938*, San Antonio, Texas, 1997.
9. Blom, S.M.P., Hagoort, J., *"The Combined Effect of Near-Critical Relative Permeability and Non-Darcy Flow on Well Impairment by Condensate Drop-Out", paper SPE 39376*, Alberta, Canada, 1998.
10. Blom, S.M.P., Hagoort, J.: *"How to include the Capillary Number in Gas Condensate Relative Permeability Functions?", paper SPE 49268*, Louisiana, 1998.
11. Chowdhury, N., Sharma, R., Pope, G.A. and Sepehrnoori, K.: *"A Semianalytical Method to Predict Well Deliverability in Gas-Condensate Reservoirs",* SPE Res Eval & Eng 11 (1), 2008.
12. Deddy, A., Kaczorowski, N.J. and Better, S.: *"Production Performance of a Retrograde Gas Reservoir: A Case Study of the Arun Field", SPE* November 1994.

13. Du, Y., Guan, L. and Li, D.: *"Deliverability of Wells in the Gas Condensate Reservoir"*, *paper SPE 88796*, Abu Dhabi, U.A.E., 2004.
14. Du, Y. and Guan, L.: *"Well Deliverability Loss Analysis in the Gas Condensate Reservoir",* Canadian International Petroleum Conference 8-10 June 2004.
15. Eclipse Reference Manual, 2010.2
16. Fan, L., Harris, B.W., Jamal A.,, Kamath, J., Mott, Pope, G.A., Shandrygin, A. and Whitson, C.H.: *"Undersanding Gas-Condensate Reservoirs"*, Winter 2005/2006
17. Fevang, Ø. and Whitson, C.H.: *"Modeling Gas Condensate Well deliverability", SPE* Oct. 1995.
18. Fevang, Ø.: *"Gas Condensate Flow Behavior and Sampling", Ph.D. thesis*, The Norwegian Institute of Technology University of Trondheim, Oct. 1995.
19. In Amenas Development Plan, Dec. 2002.
20. Lal, R.R.: *"Well testing In Gas-Condensate Reservoirs", M.S. thesis,* Stanford University, 2003.
21. Lee, S.-T. and Chaverra, M.: *"Modelling and Interpretation of Condensate Banking for the Near Critical Cupiagua Field", SPE* 27-30 Sept. 1998.
22. Li, K. and Firoozabadi, A.: *"Phenomenological Modeling of Critical Condensate Saturation and Relative Permeabilities in Gas/Condensate Systems" SPE Journal*, *Vol. 5, No. 2*, June 2000.
23. Roussennac, B.: *"Gas-condensate well test analysis", M.S. thesis,* Stanford University, CA., 2001.
24. Shi, C.: *"Flow Behavior of Gas Condensate Wells", M.S. thesis,* Stanford University, 2005.
25. Singh, K. and Whitson, C.H: *"Gas Condensate Preudopressure in Layered Reservoirs" paper SPE 117930*. Abu Dhabi, U.A.E, 2008.
26. Wall, C. G.: *"Characterization of gas-condensate reservoirs and traditional production methods, North Sea Gas-condensate Reservoirs and their Development, Oyez scientific and technical service"*, pp. 1-12., 1982.
27. Whitson, C.H. and Fevang, Ø.: *"Generalized Preudopressure Well Treatment in Reservoir Simulation", IBC Conference,* 1997.
28. Whitson, C.H. and Fevang, Ø.: *"Gas Condensate Relative Permeability for Well Calculations", SPE* 3-6 Oct. 1999.

29. Whitson, C.H. and Torp, S.B.: "Evaluating Constant Volume Depletion Data," *JPT* (1983) 610-620; *Trans.*, AIME.

Nomenclature

B_o oil Formation Volume Factor (FVF), m3/Sm3

B_g gas (FVF), m3/Sm3

k absolute permeability, md

k_{rg} gas relative permeability

k_{ro} oil relative permeability

kh flow capacity

d distance, m

r radius, ft

S_o oil saturation

S_g gas saturation

S_{oc} critical oil saturation

T reservoir temperature, ºC

Abbreviations

BHFP bottom hole flowing pressure, barsa

THP tubing head pressure, barsa

OGR condensate-gas ratio, Sm3/m3

WD well deliverability

LGC lean gas condensate

MGC medium gas condensate

RGC rich gas condensate

MPF Multiphase Pseudopressure Function

Symbols

μ_g gas viscosity, cP

μ_o oil viscosity, cP

Appendix A

Appendix A.1. Black-Oil properties

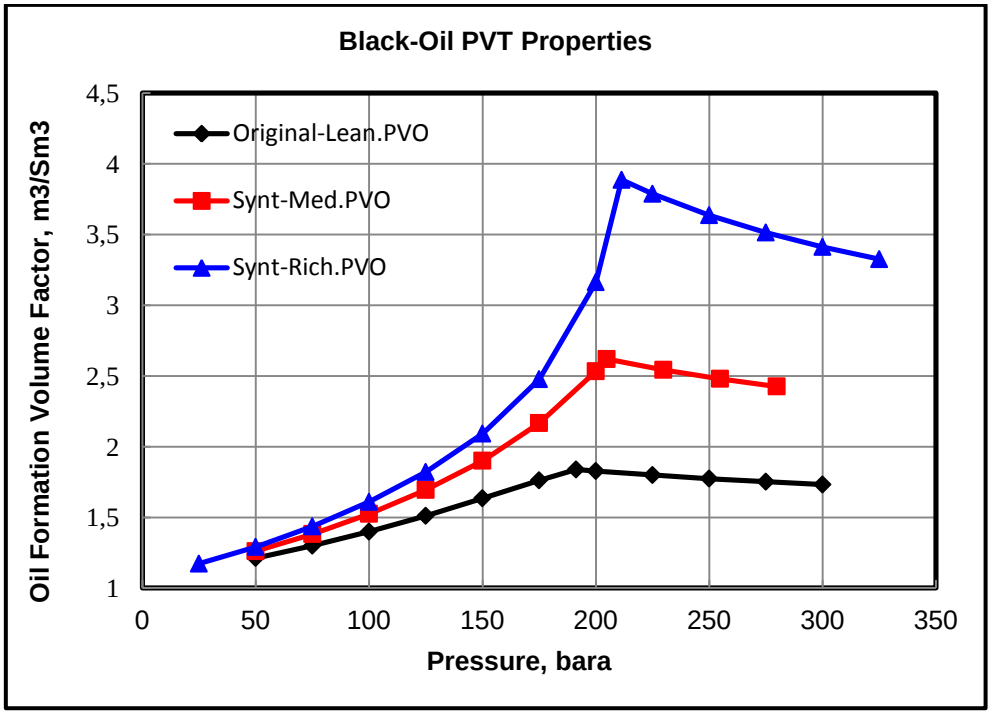

Fig. A.1.1: Oil Formation Volume Factor vs. pressure

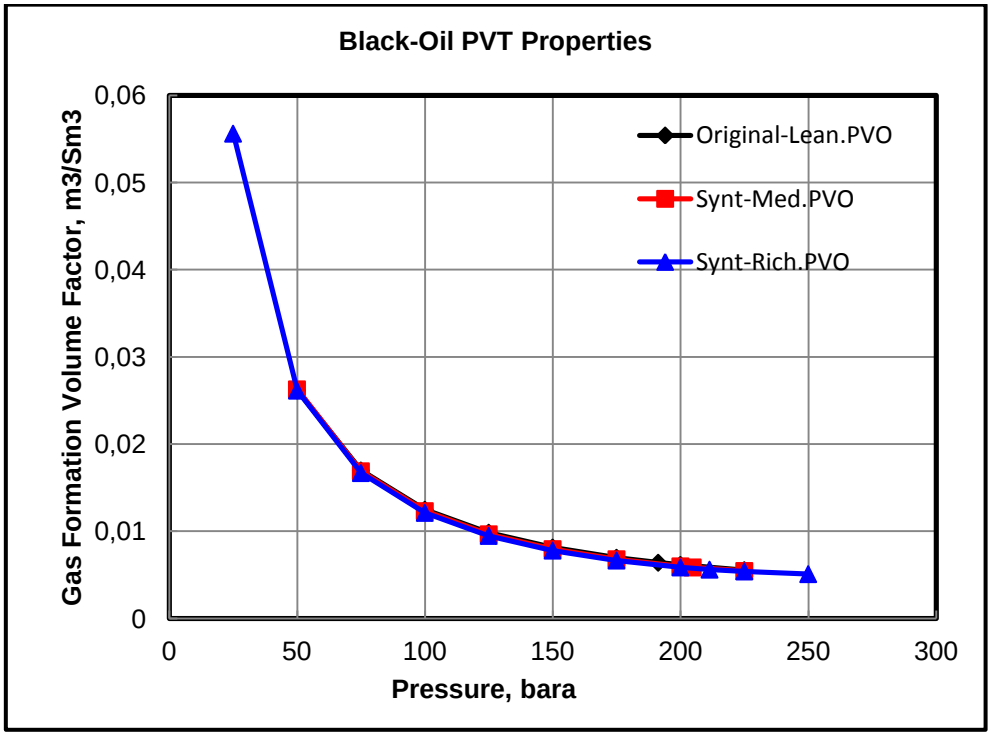

Fig. A.1.2: Gas Formation Volume Factor vs. Pressure

Appendix A.2. The Comparison of THPs in WPI Mult approach

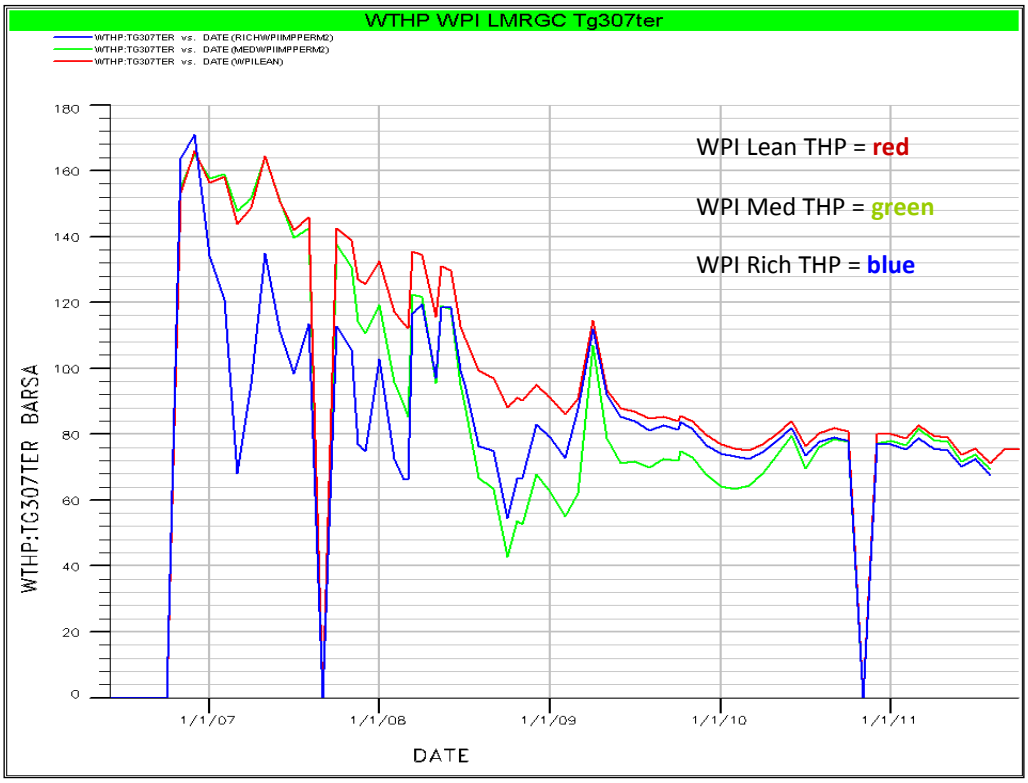

Fig. A.1.3: The THPs of WPI Mult approach for lean, medium and rich GC, Tg307ter

Appendix B

Appendix B.1. Tg307ter Medium simulation result

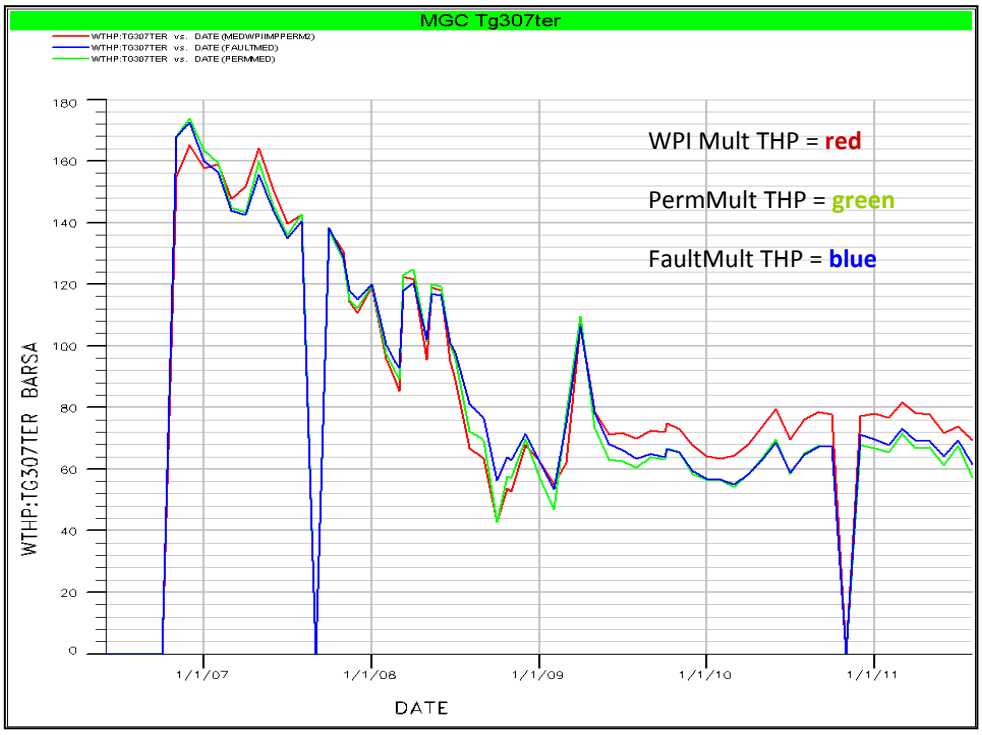

Fig. B.1.1: The comparison of THP of WD approaches, Tg307ter, MGC

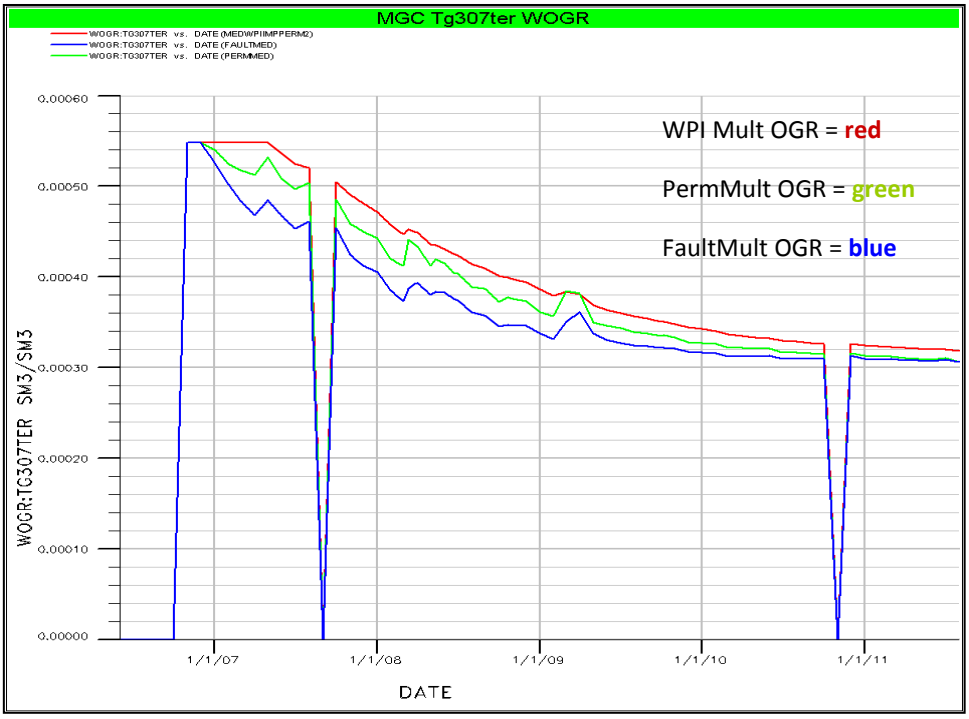

Fig. B.1.2: The flowing OGR profile of WD approaches, Tg307ter, MGC

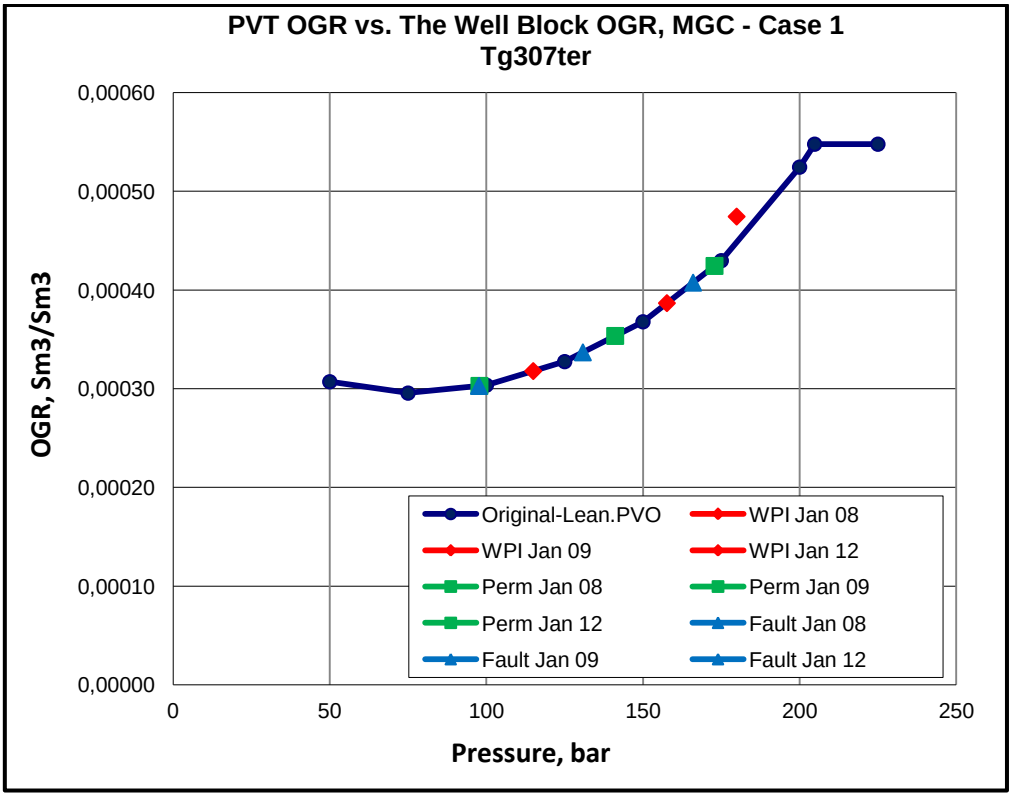

Fig. B.1.3: The input PVT OGR and the well grid OGR vs. pressure, Tg307ter, MGC

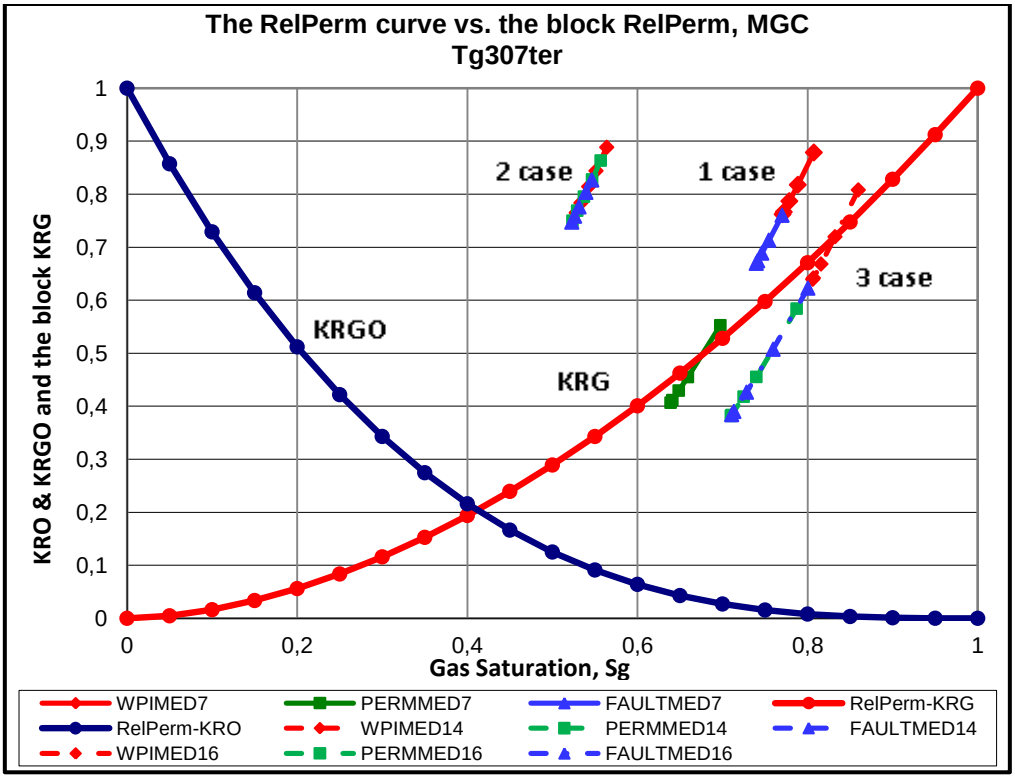

Fig. B.1.4: The input RelPerm curve and the well grid KRG vs. Sg, Tg307ter, MGC

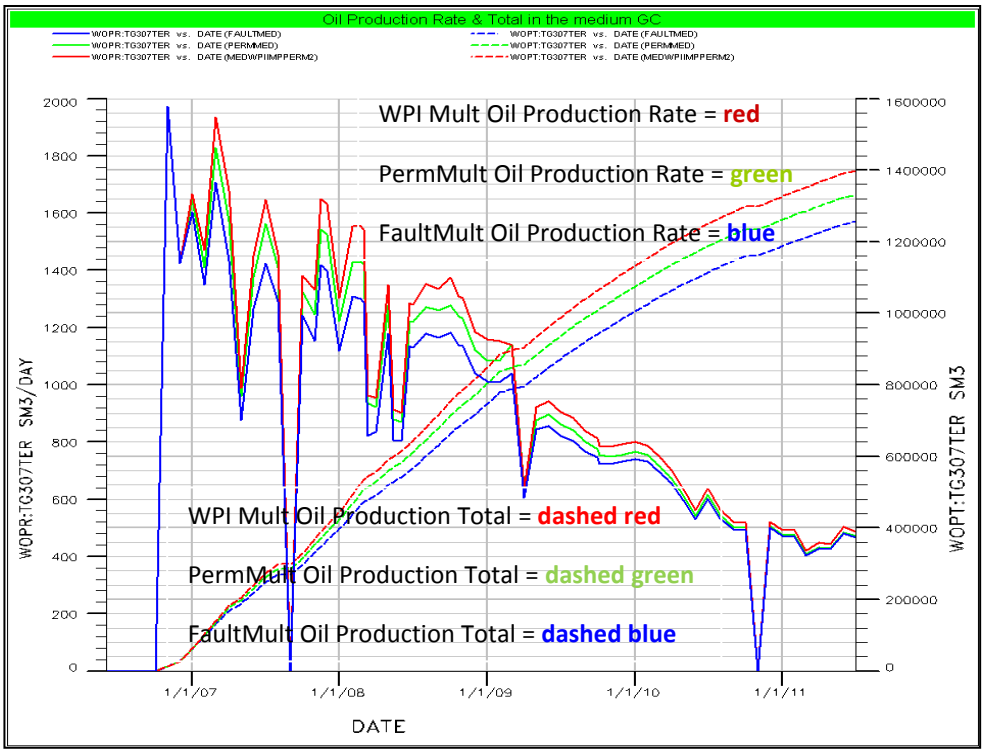

Fig. B.1.5: The oil production rate and total of WD approaches vs. time, Tg307ter, MGC

Appendix B.2. Tg307ter Rich GC simulation result

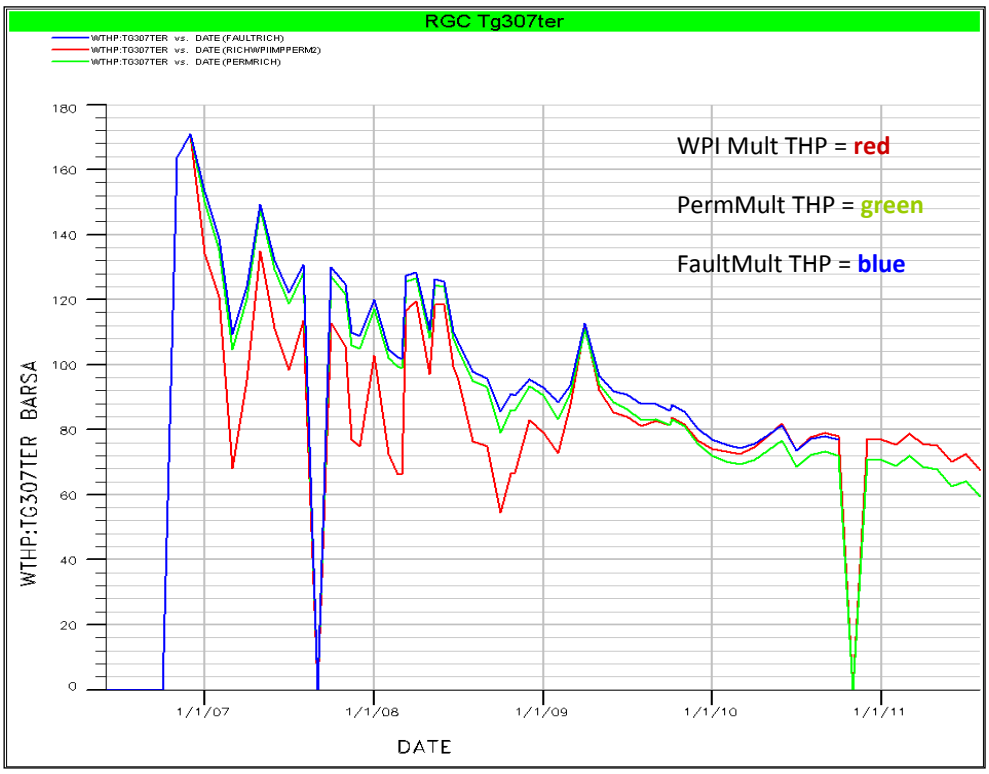

Fig. B.2.1: The comparison of THP of WD approaches, Tg307ter, RGC

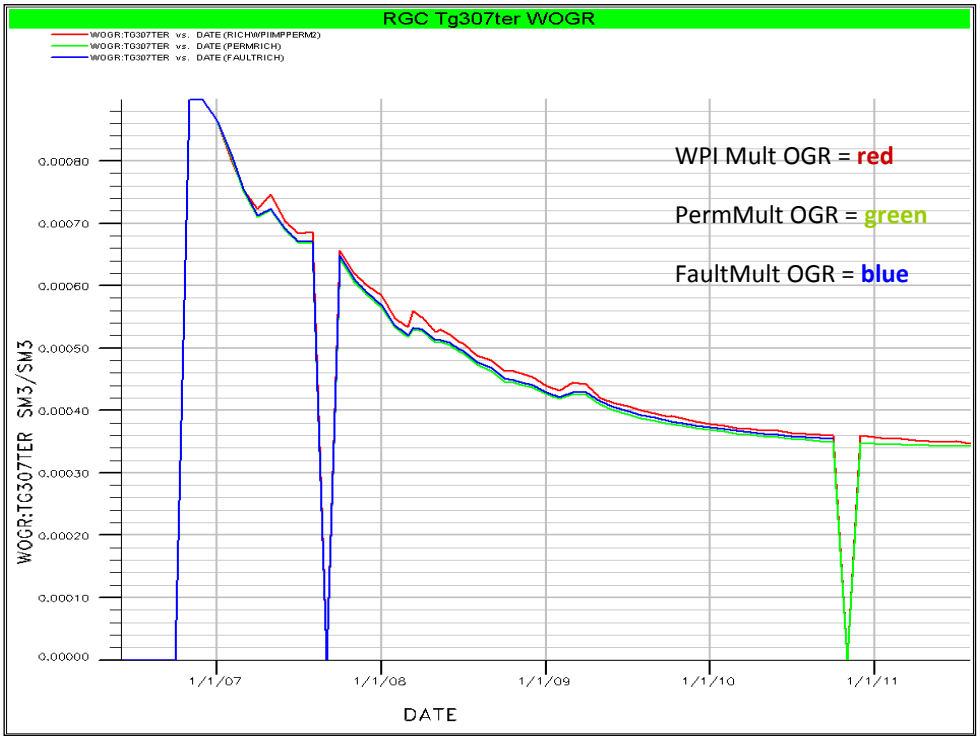

Fig. B.2.2: The flowing OGR profile of WD approaches, Tg307ter, RGC

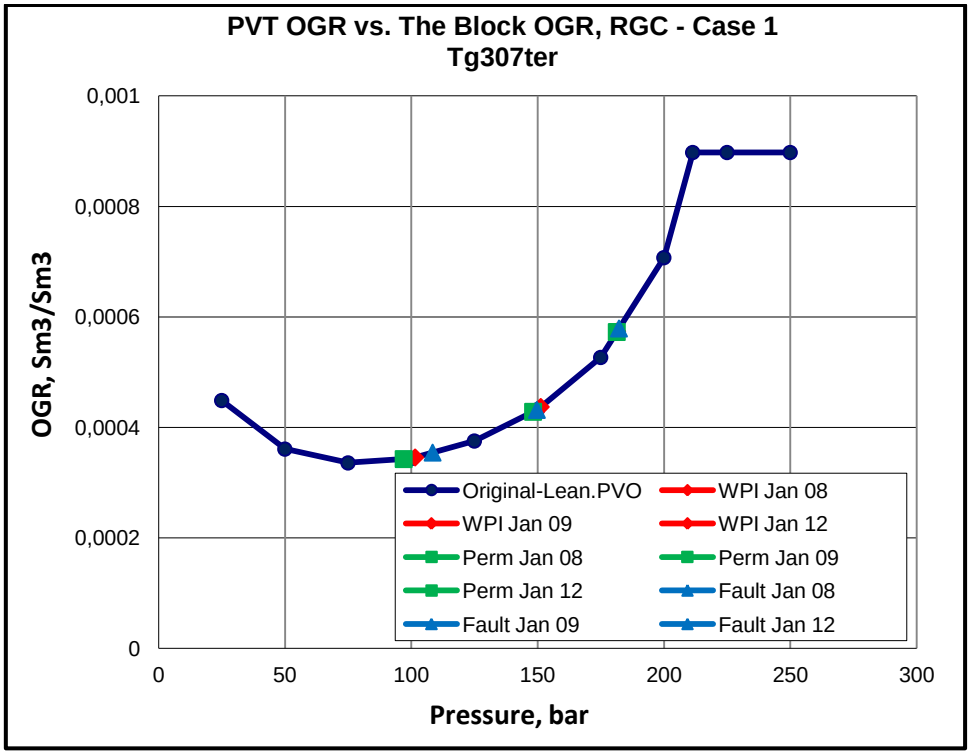

Fig. B.2.3: The input PVT OGR and the well grid OGR vs. pressure, Tg307ter, RGC

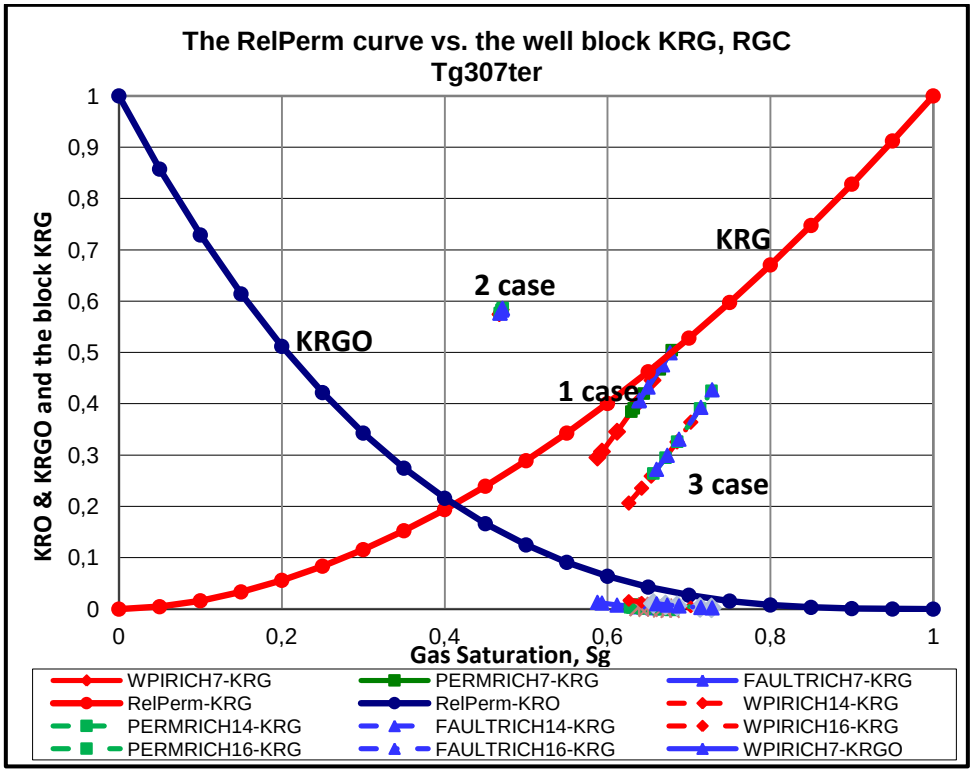

Fig. B.2.4: The input RelPerm curve and the well grid KRG vs. Sg, Tg307ter, RGC

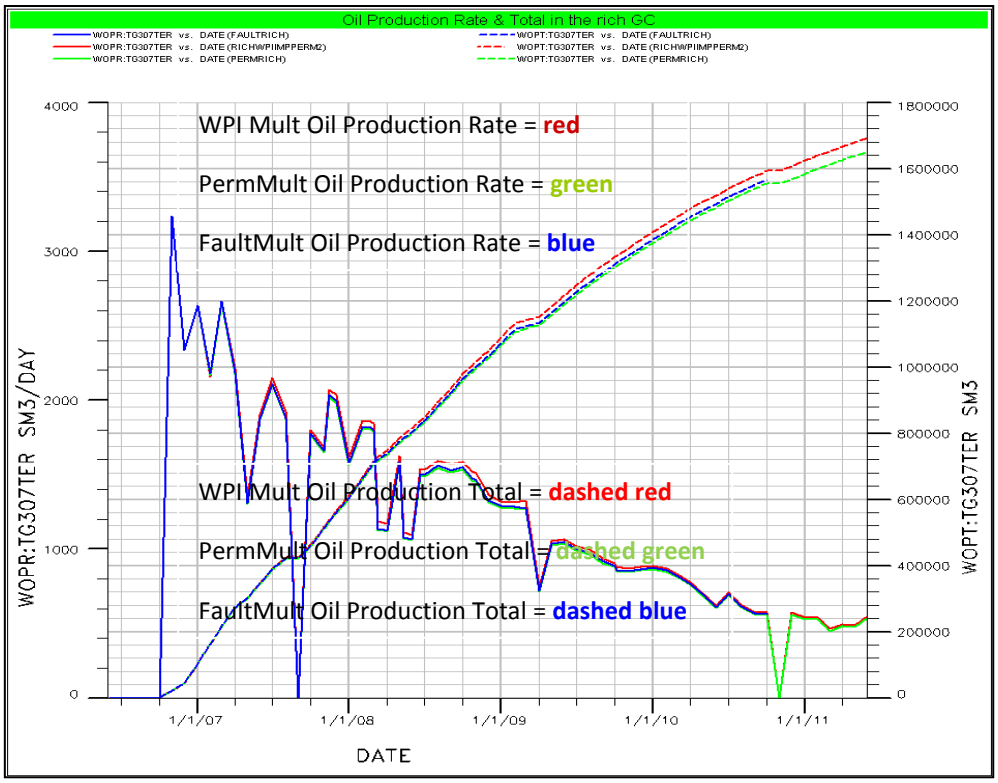

Fig. B.2.5: The oil production rate and total of WD approaches vs. time, Tg307ter, RGC

Appendix C

Appendix C.1. Tg303bis Medium simulation result

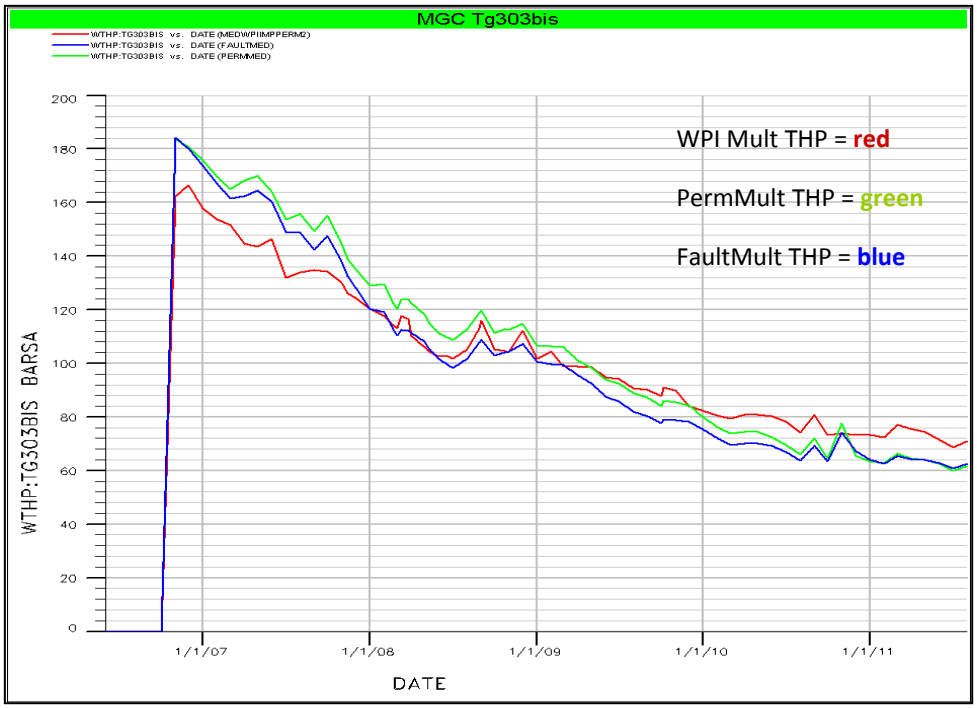

Fig. C.1.1: The comparion of THP of WD approaches, Tg303bis, MGC

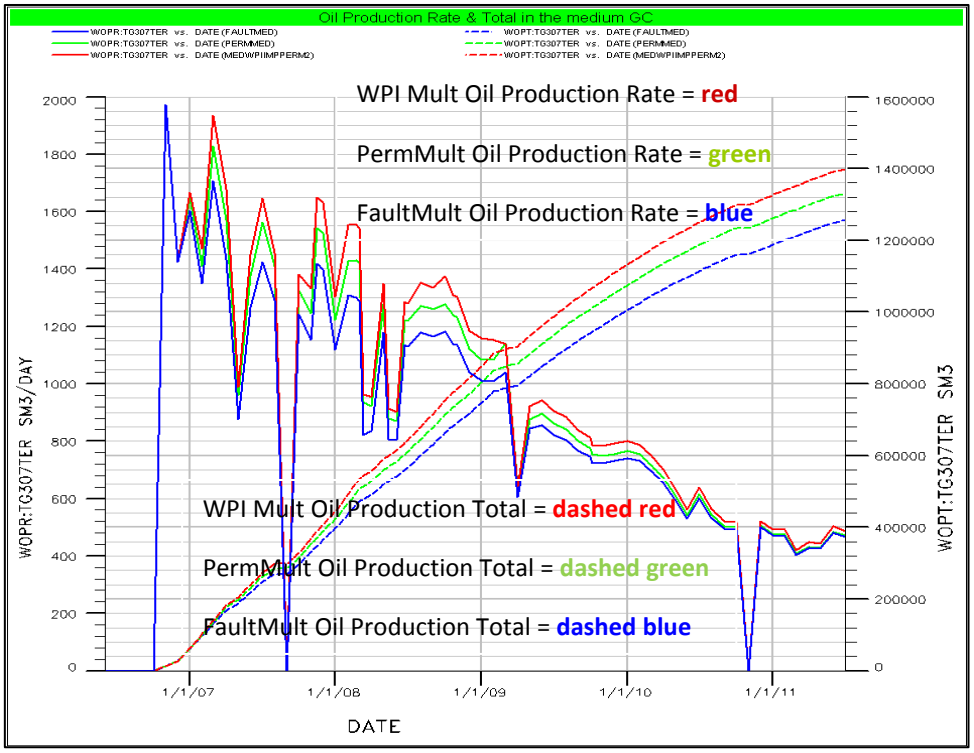

Fig. C.1.2: The oil production rate and total of WD approaches vs. time, Tg303bis, MGC

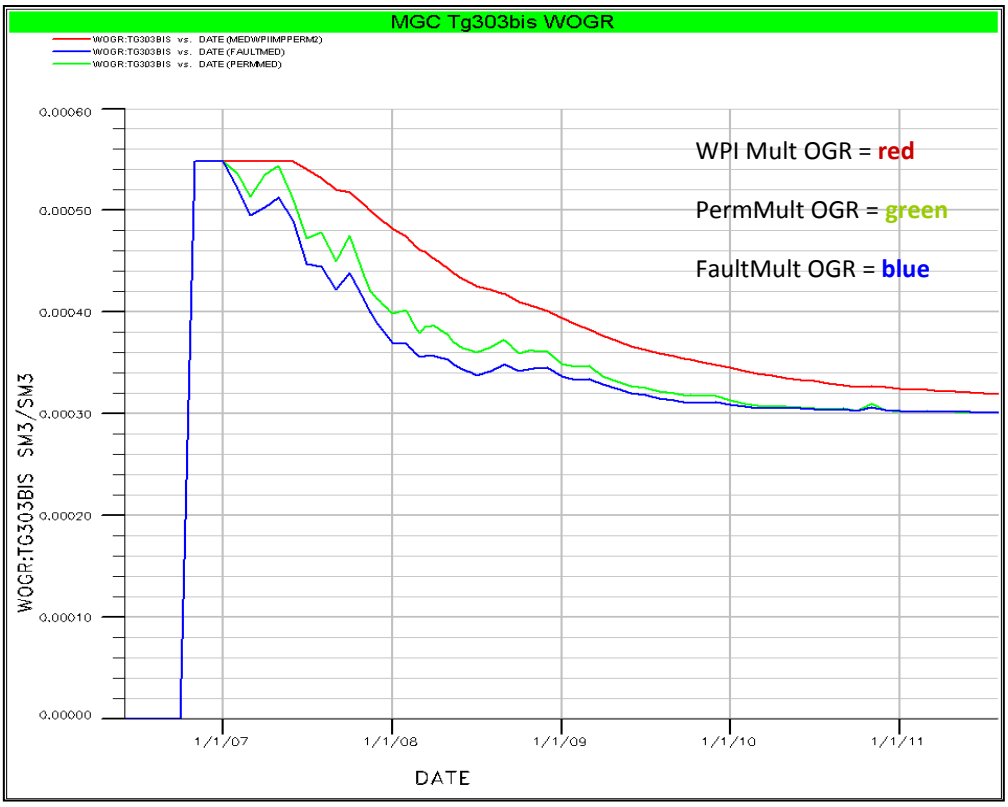

Fig. C.1.3: The flowing OGR profile of WD approaches, Tg303bis, MGC

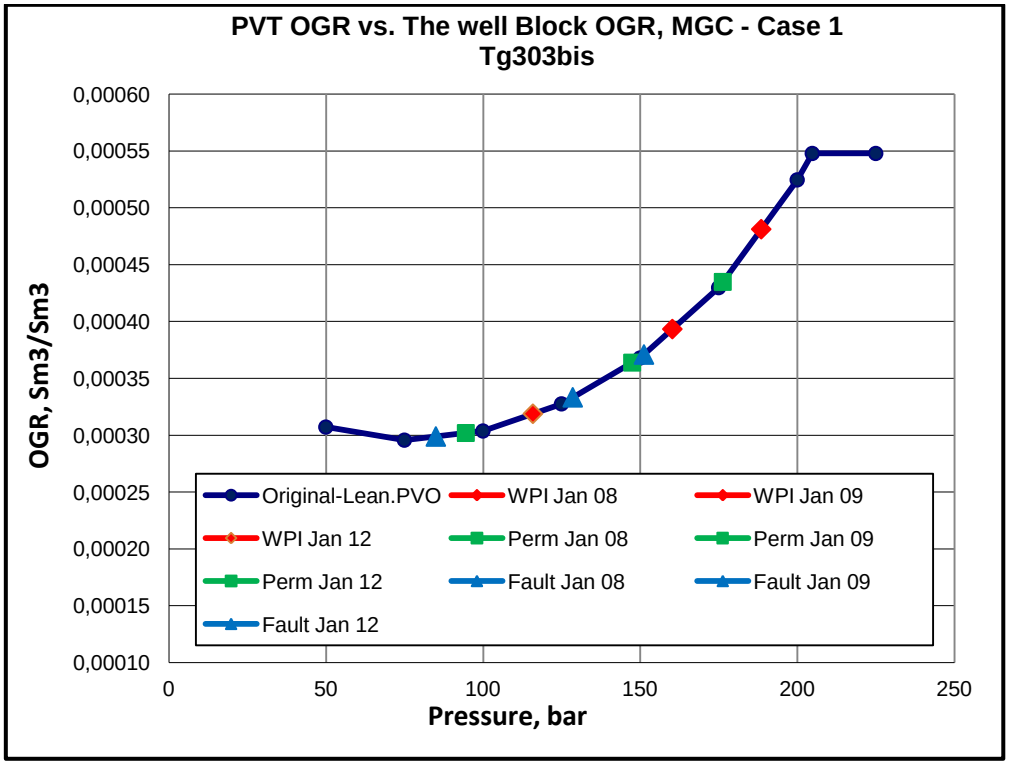

Fig. C.1.4: The input PVT OGR and the well grid OGR vs. pressure, Tg303bis, MGC

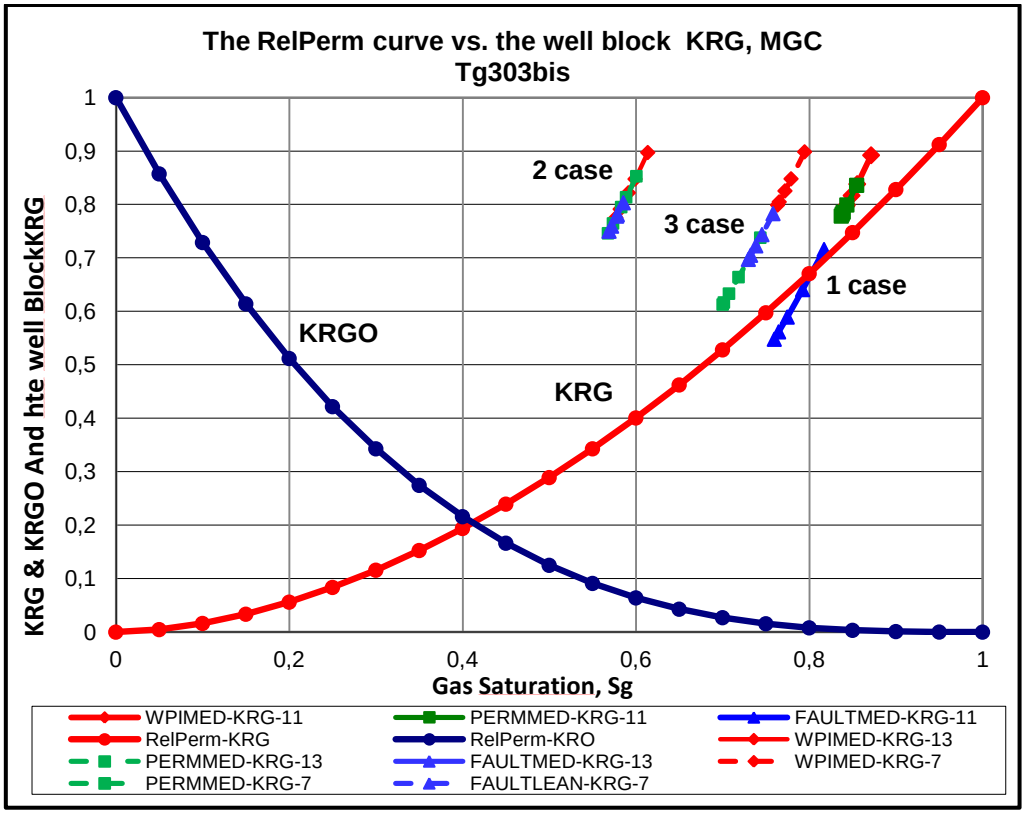

Fig. C.1.5: The input RelPerm curve and the well grid KRG vs. Sg, Tg303bis, MGC

Appendix C.2. Tg303bis Rich GC simulation result

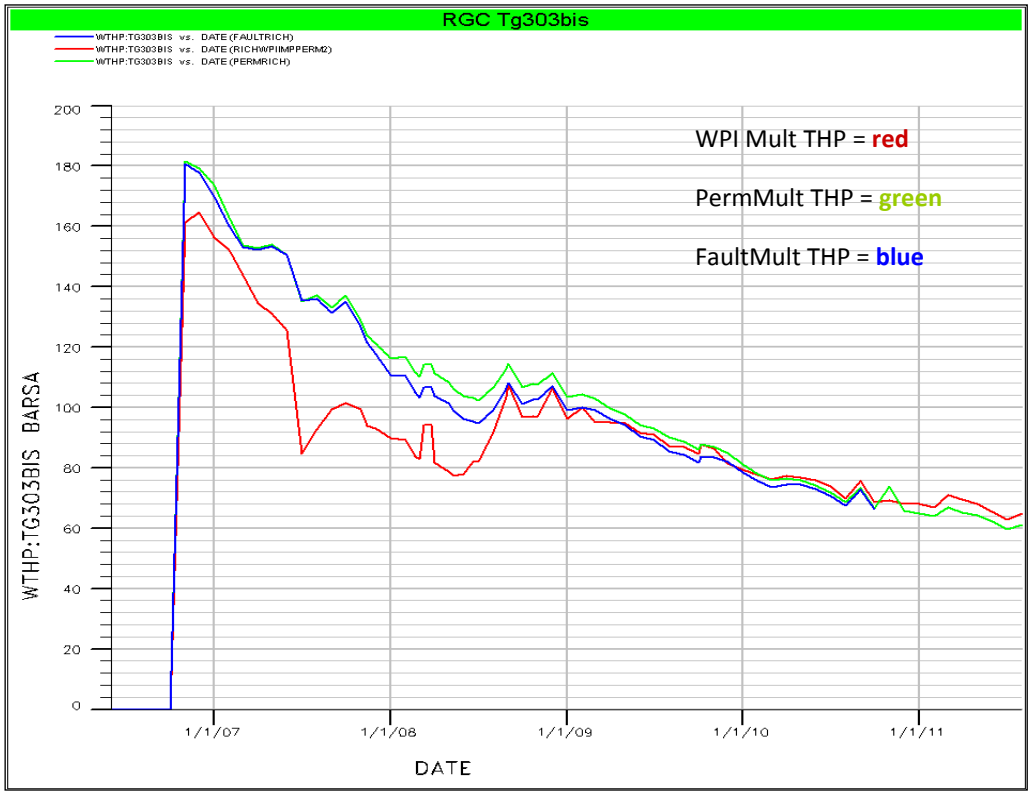

Fig. C.2.1: The comparison of THP of WD approaches, Tg303bis, RGC

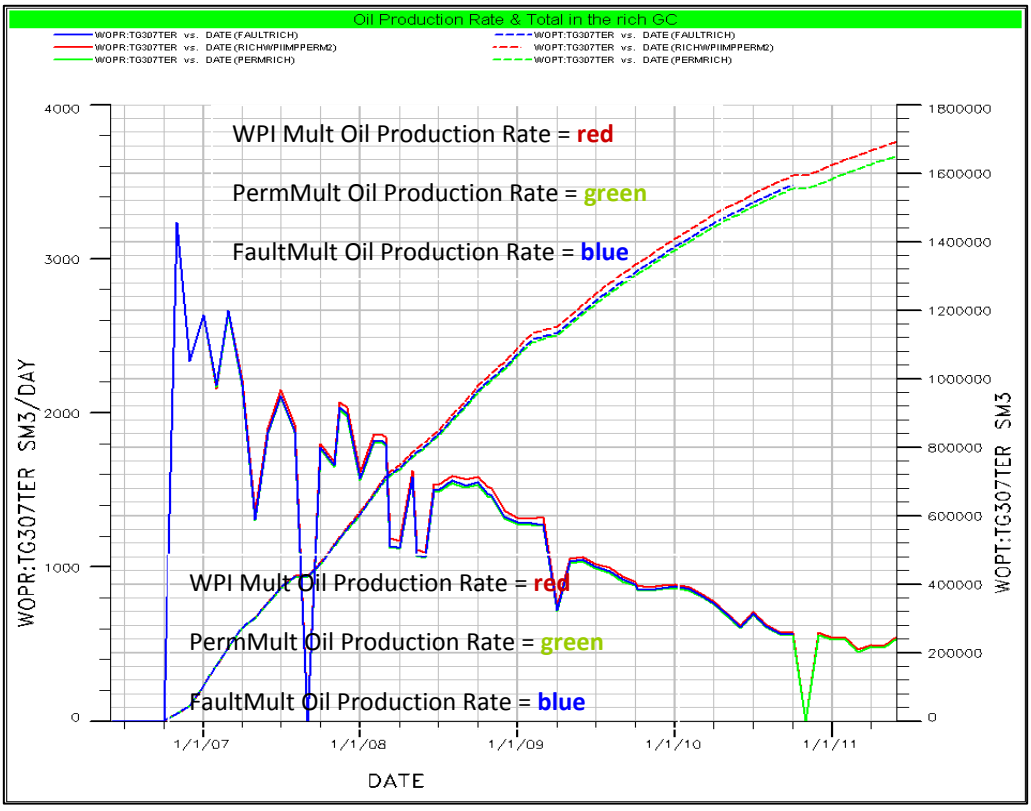

Fig. C.2.2: The oil production rate and total of WD approaches vs. time, Tg303bis, RGC

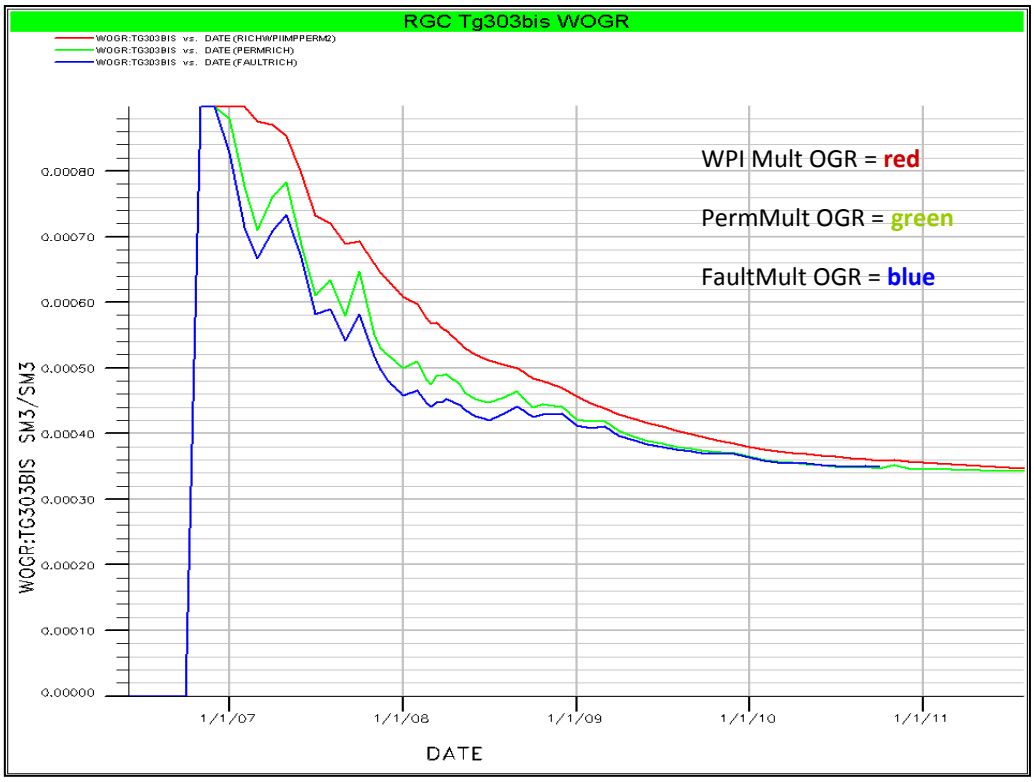

Fig. C.2.3: The flowing OGR profile of WD approaches, Tg303bis, RGC

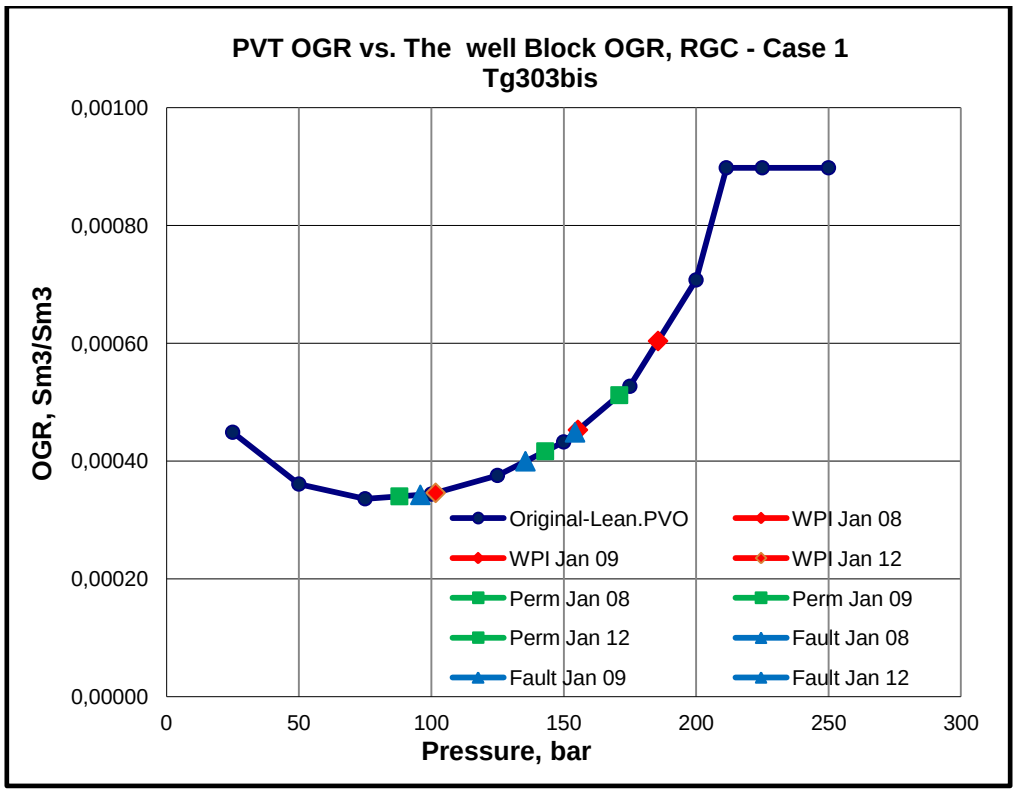

Fig. C.2.4: The input PVT OGR and the well grid OGR vs. pressure, Tg303bis, RGC

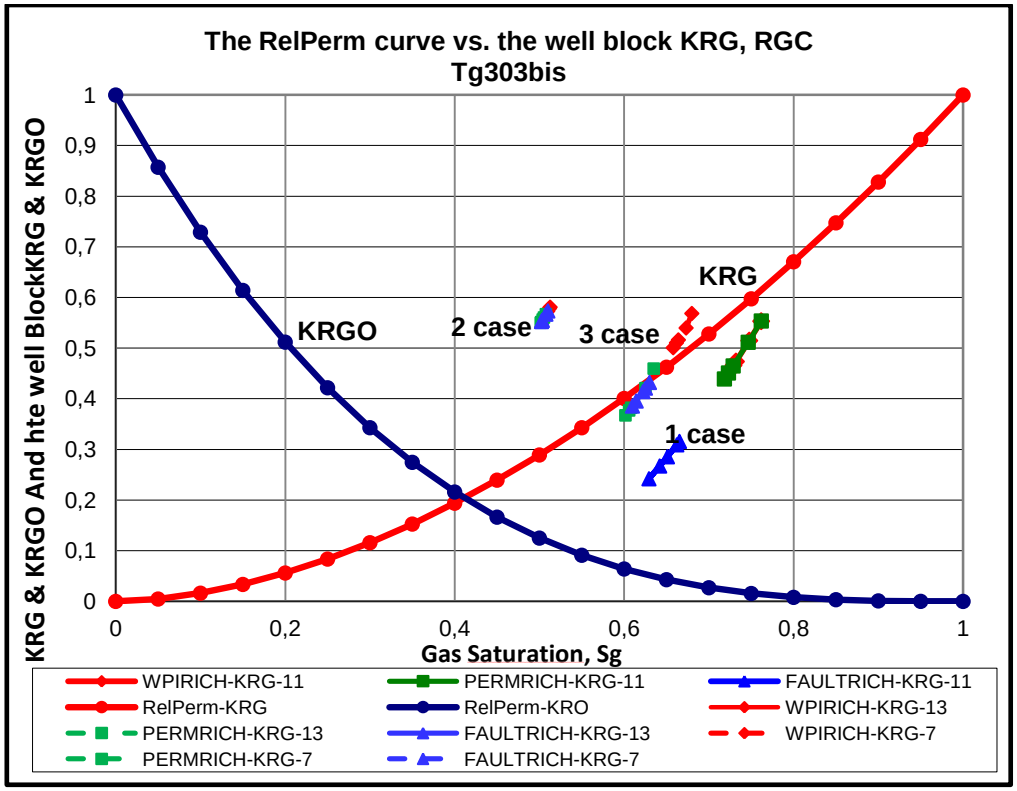

Fig. C.2.5: The input RelPerm curve and the well grid KRG vs. Sg, Tg303bis, RGC